Declassified per 31 DEC 62 memo of Dutt Sec. Manual

CONFIDENTIAL

Office of Scientific Research and Development

National Defense Research Committee

Division Six. Section 6.1

FINAL REPORT - CONTRACT OEMsr-207

DEVELOPMENT OF THE HIGH SPEED WATER TUNNEL AND SUMMARY OF RESULTS

by

California Institute of Technology

Pasadena, California

OSRD No.

Section No. 6.1-sr207-2351

August 31, 1945

Copy No. 146

CONFIDENTIAL

Office of Scientific Research and Development
National Defense Research Committee
Division Six - Section 6.1

FINAL REPORT - CONTRACT OEMsr-207

DEVELOPMENT OF THE HIGH SPEED WATER TUNNEL

AND SUMMARY OF RESULTS

Submitted for California Institute of Technology under Contract OEMsr-207

By Robert T. Knapp
Official Investigator

Approved for distribution

By _____
Chief of Division 6

by

California Institute of Technology
Pasadena, California

OSRD No.

Section No. 6.1-sr207-2351

August 31, 1945

Copy No. 146

TABLE OF CONTENTS

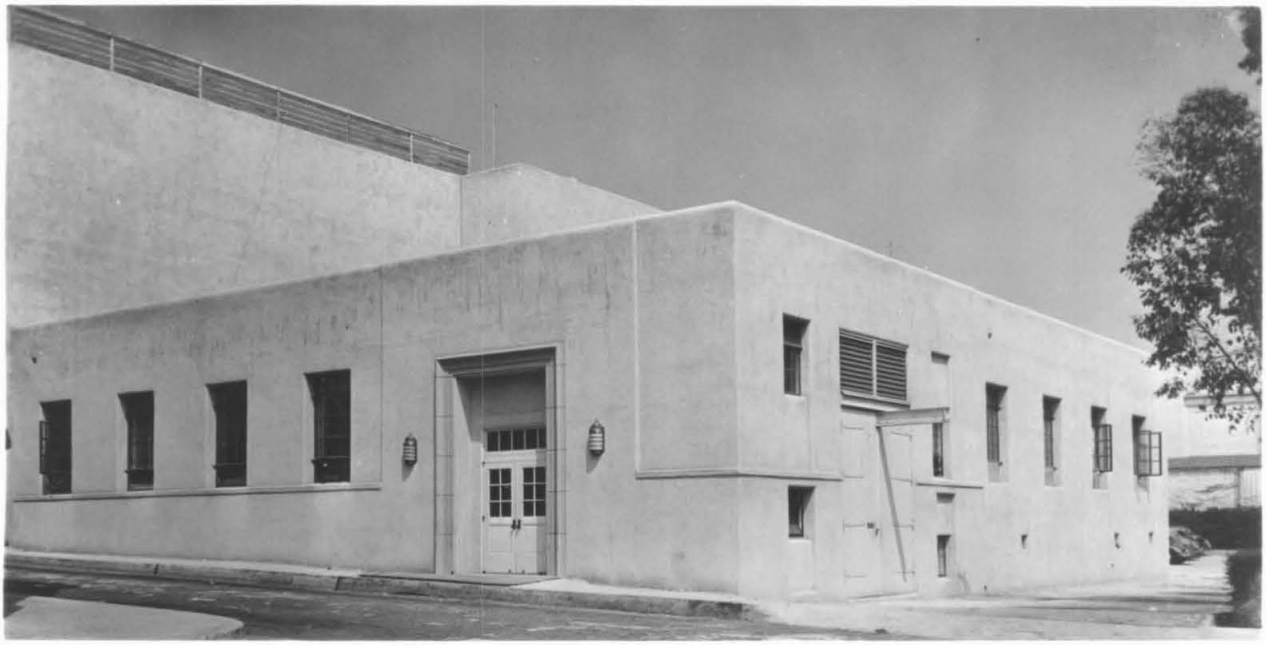

HYDRODYNAMICS LABORATORY BUILDING

DEVELOPMENT OF THE HIGH SPEED WATER TUNNEL

AND SUMMARY OF RESULTS

SUMMARY

Contract OEMsr-207 has been a project operated under Section 6.1 of the National Defense Research Committee. It has been under the general supervision of Dr. John T. Tate, Chief of Division 6, and the detailed supervision of Dr. E. H. Colpitts, Chief of Section 6.1. Under this contract, studies have been carried out under Navy Projects NO-141, NO-176, NO-149 and NO-157, and Army Projects OD-99 and AC-70. In addition, studies have been made directly for Contract OEMsr-418 operating under Division 3 of the National Defense Research Committee, Columbia University, Division of War Research, operating under Division 6, and for other projects as authorized by Division 6.

Nearly all of the projects studied have involved the determination of the hydrodynamic forces acting upon projectiles in flight, either in the air or under water. The initiating problem was the study of the streamlined depth charge for the New London Laboratory. Subsequent projects broadened the field of the Laboratory work to include rockets, bombs, mortars, shells, and torpedoes.

The purpose of this report is to present a brief review of the work carried out by the California Institute of Technology under Contract OEMsr-207 for Section 6.1 of the National Defense Research Committee. This summary includes a review of the types of problems assigned to the project, a description of the equipment developed to make the measurements required for the solution of these problems, a brief resume of the work that was completed by the projects, and a short survey of the present state of the field, including the problems that deserve further study.

PROBLEMS

With very few exceptions, the problems assigned to the Laboratory have been in the field of the exterior ballistics of projectiles. The majority of Laboratory assignments have required the measurement of the hydrodynamic forces acting on projectiles in flight. The projectiles that have been studied in the Laboratory have been of four general types: Rockets, aircraft bombs, depth charges, and torpedoes. Most of the measurements have been taken for steady conditions, i.e., for the normal operating state, although investigations have also been made on the transient forces which act under non-steady conditions. The Hydrodynamics Laboratory, in which this project has been carried out, uses water as the fluid medium with which the experimental measurements are made.

Nevertheless, in the early stages of the project it was shown that the results obtained in the Laboratory were applicable to air-flight as well as to water-flight projectiles, as long as the air-flight applications were restricted to cases in which the projectile velocities were sufficiently low so that the air could be treated as an incompressible fluid. Roughly speaking, this meant that air-flight projectiles having velocities below 700 feet per second could be studied in the Laboratory with the assurance that the measurements would have an acceptable accuracy.

HISTORY OF PROJECT

The inception of this project can be traced to the requirements of the New London Laboratory, Columbia University, Division of War Research. In 1941, this Laboratory was studying the broad aspects of the antisubmarine program. In the summer of 1941, the New London Laboratory became interested in the development of a streamlined depth charge, which would have a much higher fall velocity in water than the conventional type of depth charge in use at that time. It soon became evident that in order to design successful projectiles of this type, it would be necessary to know their hydrodynamic characteristics. Although it was believed that many of these characteristics could be determined satisfactorily in a wind tunnel, it was felt that certain important phenomena, such as cavitation, could not be studied by this means. Furthermore, it was found that existing wind tunnels had very heavy programs of their own and that it would be unwise to depend upon obtaining the use of such facilities for a rush program. Therefore, in August 1941, it was proposed by Robert T. Knapp, Associate Professor of Hydraulic Engineering at the California Institute of Technology, who was acting as consultant in hydrodynamics to T. E. Shea, Director of the New London Laboratory, that the Laboratory sponsor the construction of a small water tunnel for use in measuring the hydrodynamic forces on projectiles. This proposal resulted in the recommendation by Mr. Shea to Dr. John T. Tate and Dr. E. H. Colpitts of Division 6 of the National Defense Research Committee, that the NDRC should sponsor the construction of such a water tunnel at the California Institute of Technology under a direct NDRC contract. Such an arrangement was initiated by a letter of intent dated October 15, 1941. The project was assigned to the Hydraulic Machinery Laboratory because of the large amount of equipment located there which could be adapted to this new use. A small staff was immediately organized, and design and construction started. The tunnel was put into operation early in the spring of 1942. It has been in continuous operation from that time to the termination of the contract at the end of August 1945. A rough idea of the development of the project is given by growth of the staff, as shown graphically in Figure 1.

The first projectile studied in the tunnel was the streamlined depth charge being developed by the New London Laboratory. Before the work on this was completed it became desirable to develop a low drag, stable instrument case to house some equipment to be towed by cable from airplanes. The assignments were then

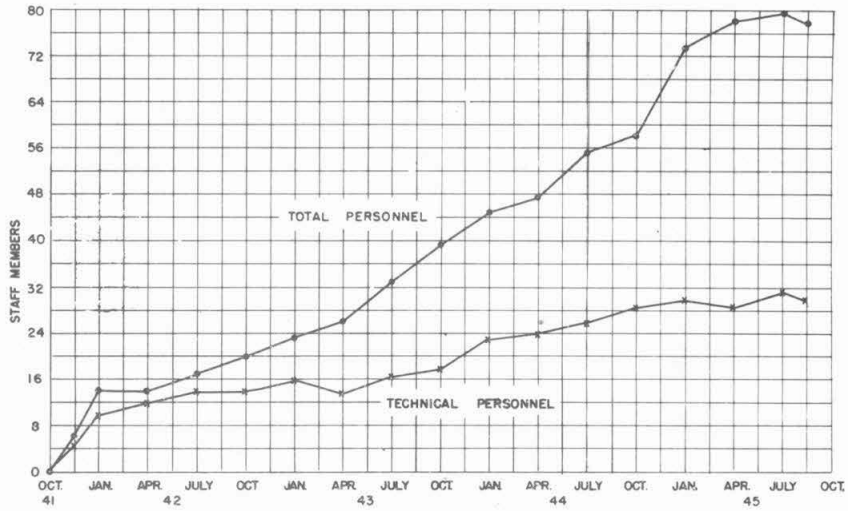

FIG. 1 – GROWTH OF PROJECT STAFF

expanded to include studies of a series of rocket projectiles for the Ordnance Department of the Army through contacts with the Ballistic Research Laboratory at Aberdeen Proving Ground. These rockets included the Bazooka and the 4.5-inch with folding fins. Studies were also made to improve the stability of small mortar projectiles for the same organization. Measurements were also started on the first of a long series of torpedoes. This represented an important step in the program because the torpedo with its controlled depth and course rudders and with its propulsion system presented many more problems than did the other projectiles tested. Another important expansion of the program was introduced with the torpedo studies, namely the investigation of cavitation phenomena and their relation to the production of noise by underwater projectiles. Close liaison was always maintained with the rocket program being carried out for Division 3 of the National Defense Research Committee by the California Institute of Technology under Contract OEMsr-418. Measurements have been made both on air-flight rockets and depth charges of the "mousetrap" type for this Division 3 project. Close liaison has also been maintained with the David Taylor Model Basin of the Bureau of Ships. One interesting investigation was undertaken at the request of the Basin – the study of the force and cavitation characteristics of a two-dimensional airfoil section.

In the latter half of 1943, the aircraft torpedo became a major part of the program of the Laboratory. The problems involved in the entry of the aircraft torpedo into the water and its behavior from the point of impact to the beginning of the steady run included forces and phenomena that could not be studied adequately by the use of the Water Tunnel alone. Furthermore, the original staff had increased sixfold and it was becoming severely handicapped by lack of suitable working space. The project was, therefore, authorized by the National Defense Research Committee to construct a new building and two additional pieces of major

FIG. 2A — PLAN OF FIRST FLOOR OF LABORATORY

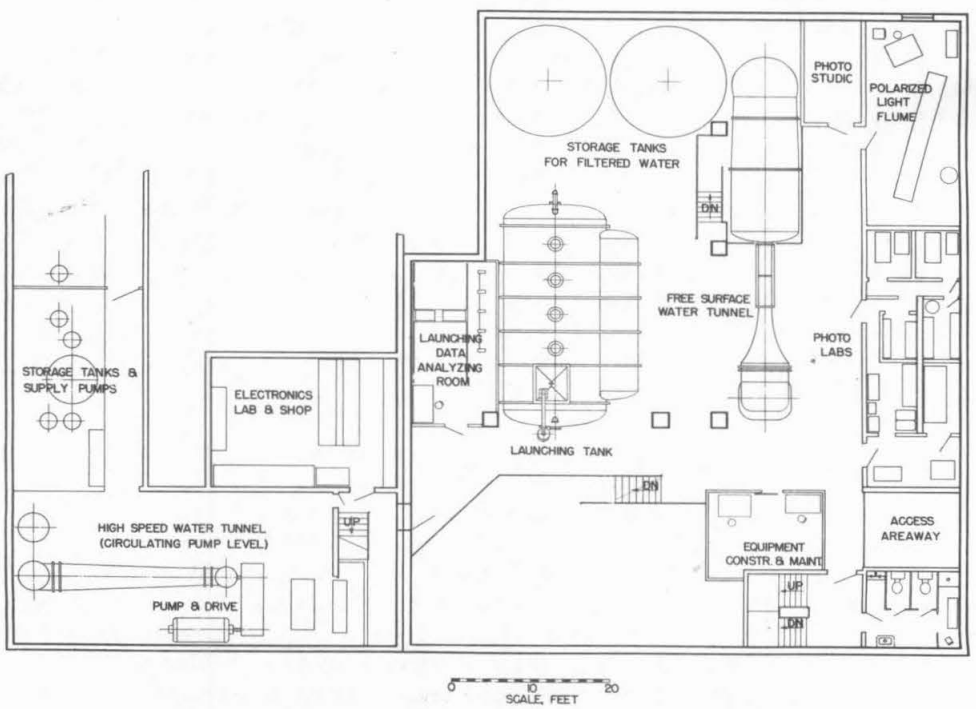

FIG. 2B — PLAN OF BASEMENT OF LABORATORY

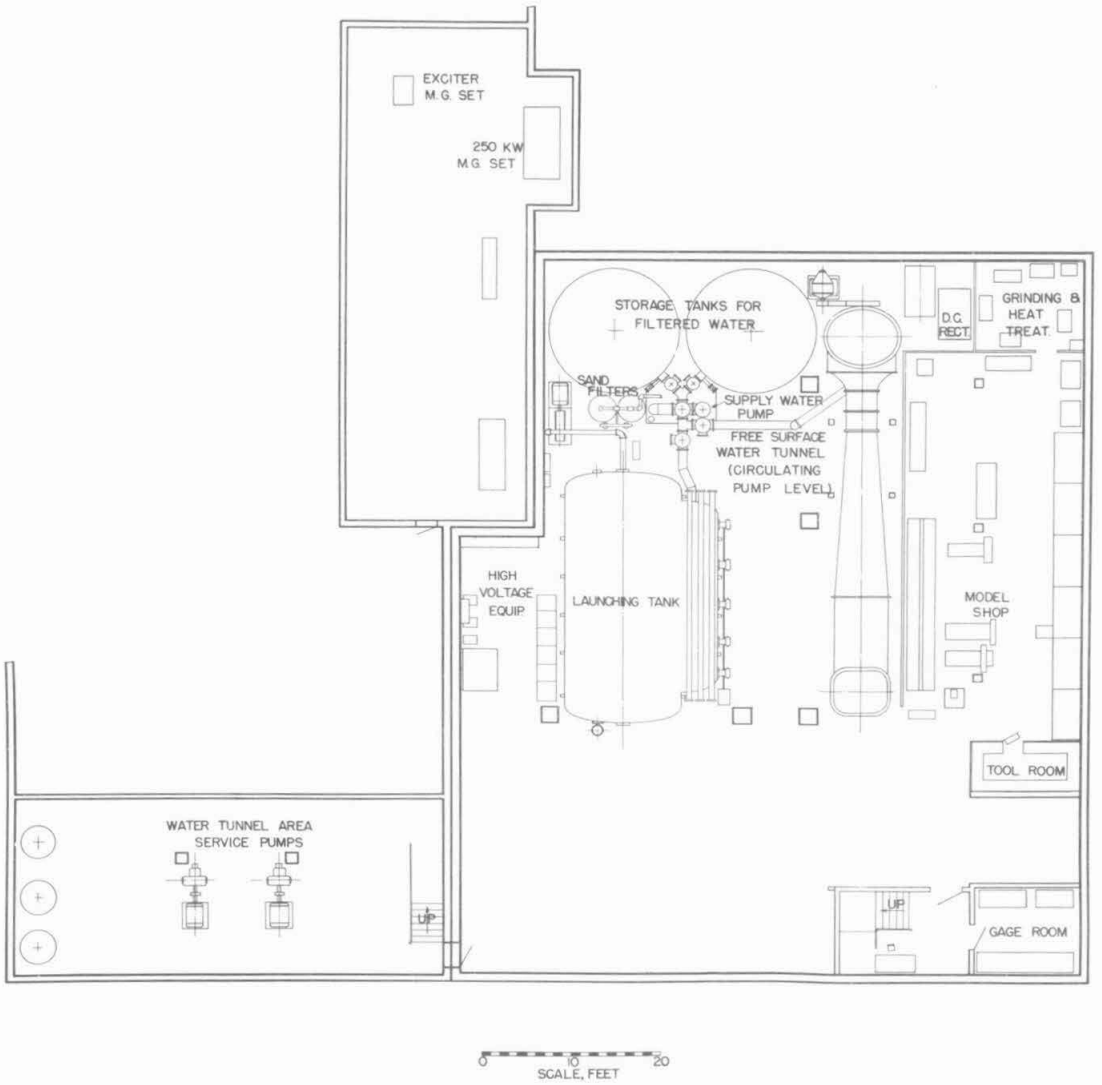

FIG. 2C — FLOOR PLAN OF SUBBASEMENT OF LABORATORY

equipment: the variable pressure launching tank and the free surface water tunnel. Construction of the building was commenced in July 1944, and it was occupied in December of the same year. Preliminary measurements were started with the launching tank in the spring of 1945. Due to the fact that top priority was assigned to the launching tank, the construction of the free surface water tunnel proceeded more slowly. Shop construction was completed and assembly commenced in August 1945.

LABORATORY

The project is housed in the new Hydrodynamics Building and the adjoining Hydraulic Machinery Laboratory. Both laboratories have three floors: the ground floor, the basement, and the subbasement. The total floor space available is approximately 19,000 square feet. Figure 2 shows the floor plan of the three floors and indicates the location of the major equipment.

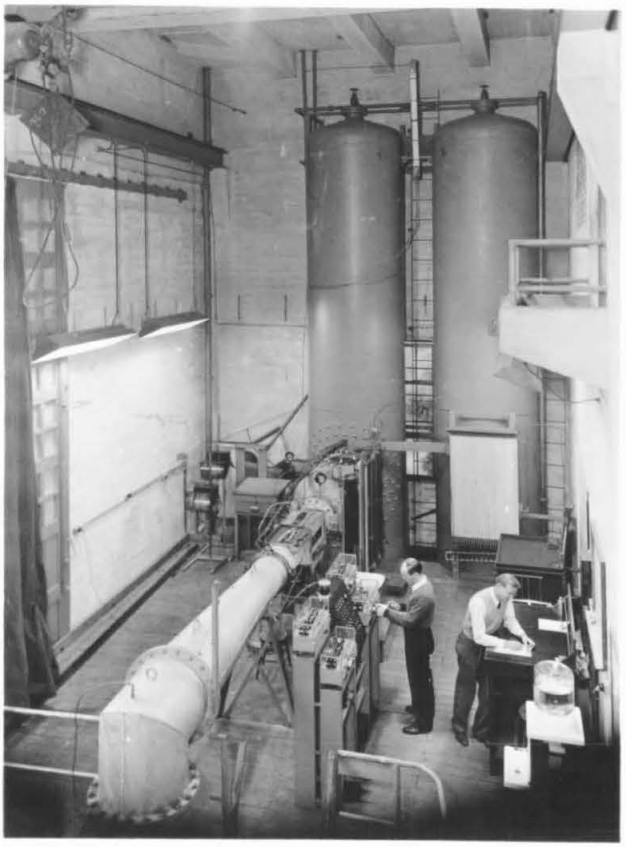

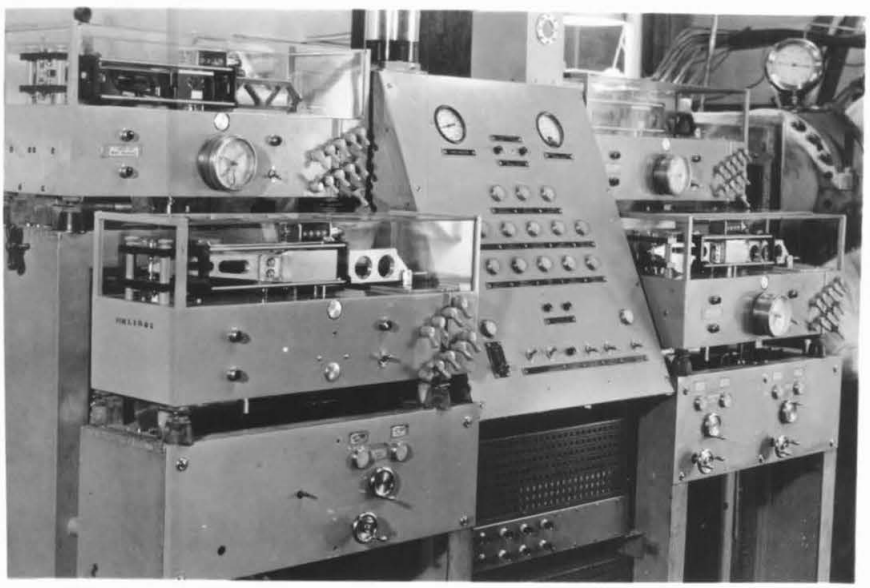

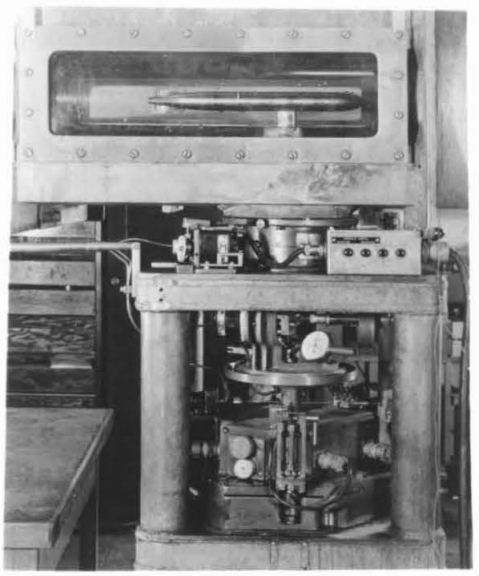

FIG. 3 – THE HIGH SPEED WATER TUNNEL AND EQUIPMENT

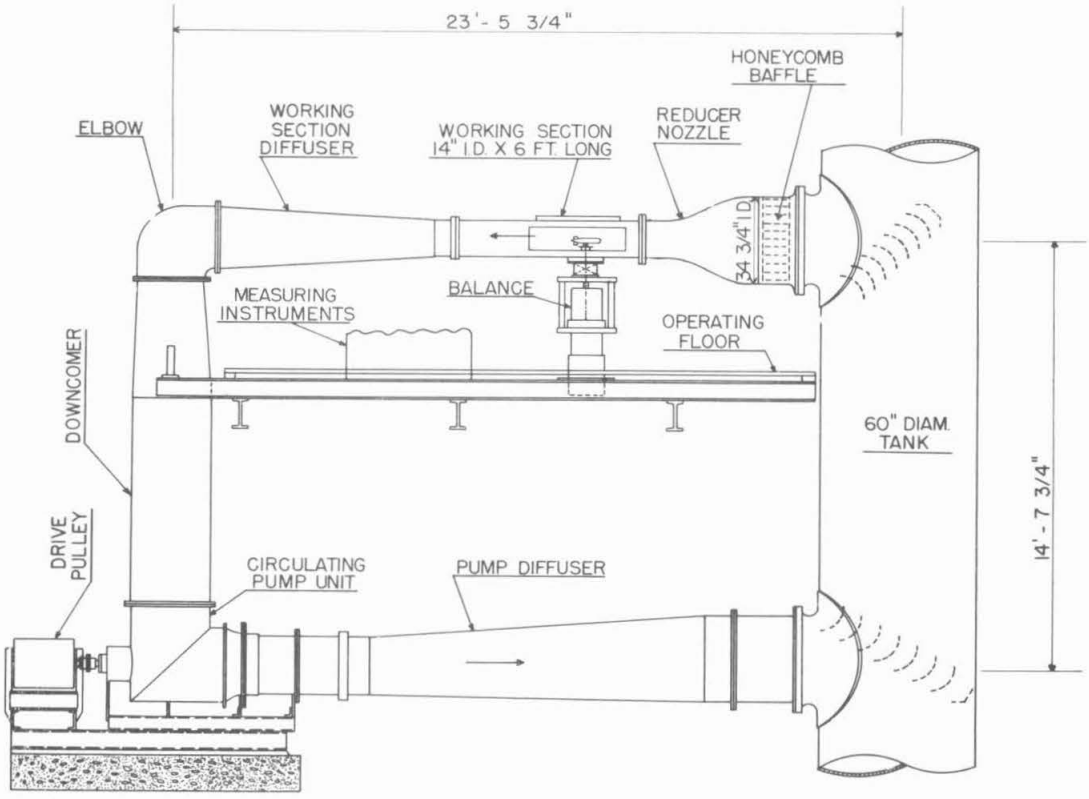

FIG. 4 — SECTIONAL ELEVATION OF HIGH SPEED WATER TUNNEL

HIGH SPEED WATER TUNNEL

The High Speed Water Tunnel is a vertical, closed-circuit channel in which water is circulated continuously by means of a propeller pump driven by a variable speed motor. Figure 3 is a photograph of the working section and measuring instruments, and Figure 4 shows the sectional elevation of this tunnel. The working section, which is 14 inches in diameter and 6 feet long, is located in the upper horizontal run of the circuit. It has the smallest cross section and, consequently, the highest velocity and the minimum pressure in the circuit. The flow velocity can be maintained at any desired value up to 70 feet per second. The models or devices to be tested are mounted in a 3-component balance of the National Physical Laboratory type. Figure 5 shows a group of the stainless steel components for 2-inch diameter models. This illustrates the type of model construction developed by the Laboratory. Measurements of the drag force, cross force, and moment can be made with the projectile parallel to the direction of flow or rotated in the horizontal plane to any desired angle between plus and minus 20 degrees from the direction of flow. The absolute pressure in the working section is controllable independent of the velocity and can be held at any desired value from three or four atmospheres down to the vapor pressure of the water. Lucite windows are provided in the working section for visual and

FIG. 5 – STAINLESS STEEL MODEL PARTS

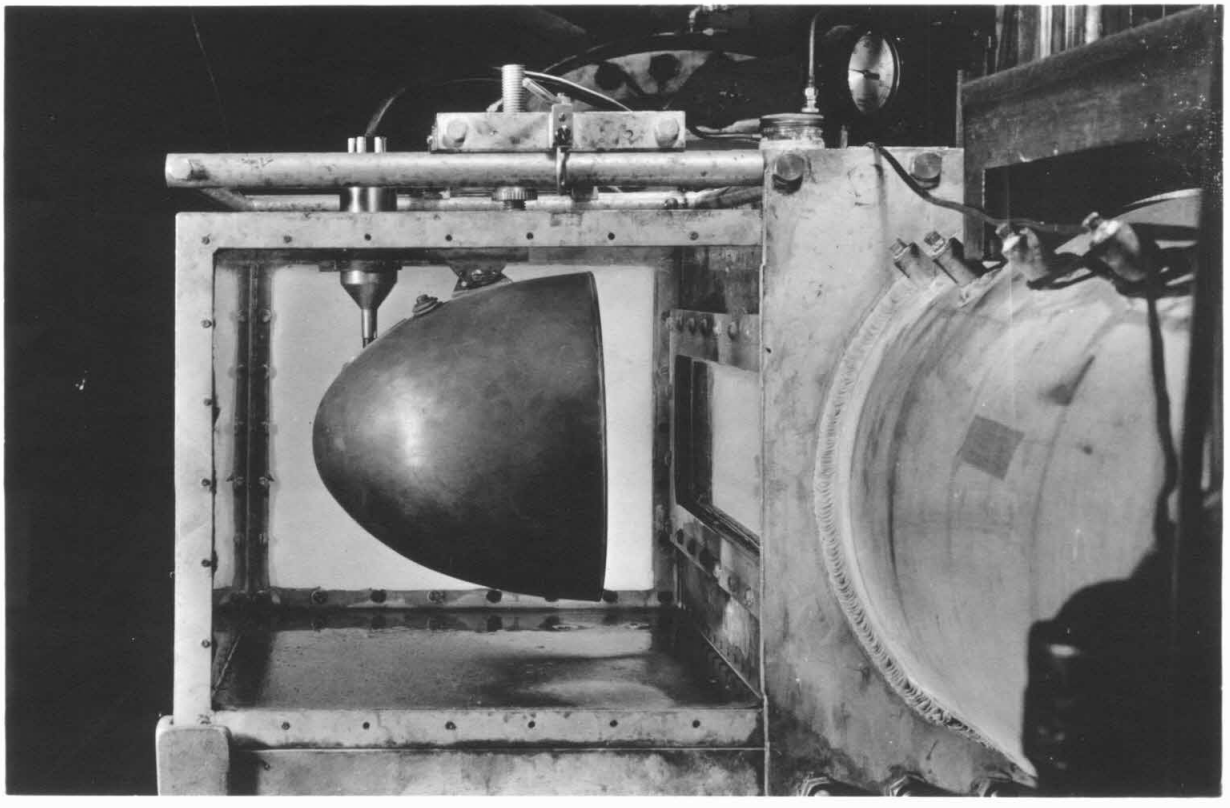

FIG. 6 – NOISE MEASURING EQUIPMENT SHOWING HORIZONTAL REFLECTORS

photographic observation. Cameras with synchronized flash lamps of the Edgerton high speed type are a regular part of the equipment. Although in the audible range the propeller pump and drive motor produce considerable noise, it has been found that the tunnel is comparatively quiet in the sound range above 6000 cycles. Therefore, microphones mounted in spherical and ellipsoidal reflectors have been developed for investigating the sounds produced by the flow passing the projectile both under cavitating and non-cavitating conditions. These reflectors have double walls enclosing an air space and are operated in a tank filled with water attached to one of the lucite windows directly opposite the model under test. These sound measurements were all made in the range above 6000 cycles. Figure 6 shows the equipment as it is installed on the working section.

Specially designed, carefully streamlined shields have been developed to support the projectile in the tunnel during high velocity cavitation tests.

It should be noted that much of the equipment used in the operation of the High Speed Water Tunnel was installed and in use in the Hydraulic Machinery Laboratory before the initiation of this project. For example, the special motor-generator set, the dynamometer used as the main drive motor, the speed control system, the constant frequency source, the storage sump, the pressure control system, the cooling system and the large vertical tank used as a part of the tunnel flow circuit were items from the former Laboratory that were incorporated with little or no change into the Water Tunnel system. Likewise, the high precision pressure gauges and manometer developed for pump and turbine tests were employed to measure the forces acting on the balance and the characteristics of the flow in the working section. If this equipment had not been available, it would have required about a year longer to have developed a working tunnel.

POLARIZED LIGHT FLUME

Many of the problems assigned to the Laboratory involved the study of specific projectile designs and the location and eradication of sources of disturbance on the surface of the projectile that produced adverse effects on the performance characteristics. To assist in this phase of the work, a small flume was constructed for the purpose of studying the flow pattern around the projectile. In order to make the flow visible, a dilute suspension of special bentonite was used instead of clear water. This form of bentonite possesses the property of streaming double refraction. If a flow of this material is viewed with transmitted polarized light, the shear pattern, and hence the velocity pattern becomes visible. Figure 7 shows a general view of this polarized light flume, Figure 8 the pattern seen through the polaroids, and Figure 9 shows typical flow pattern drawings obtained by its use. The working section in this auxiliary flume is 6 inches wide by 12 inches high and 4 feet long. Only very low velocities are used, i.e., up to about 5 feet per second.

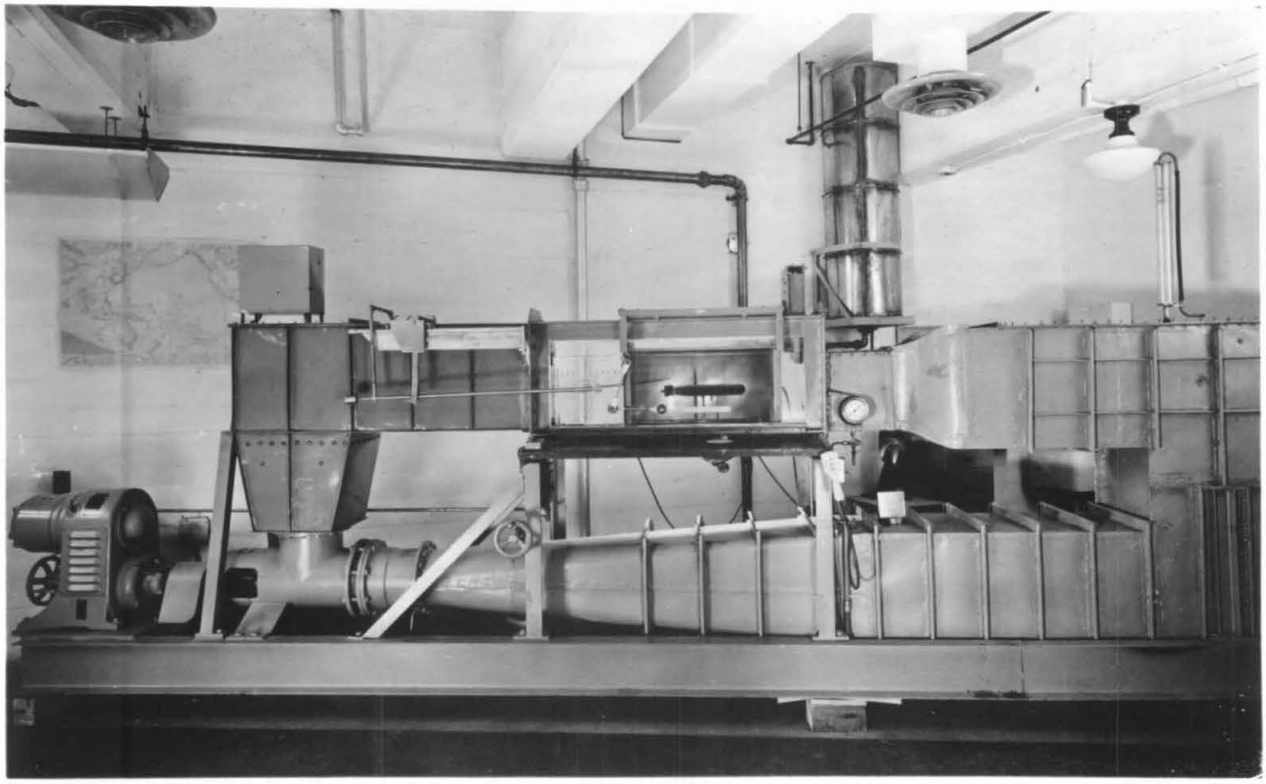

FIG. 7 – POLARIZED LIGHT FLUME

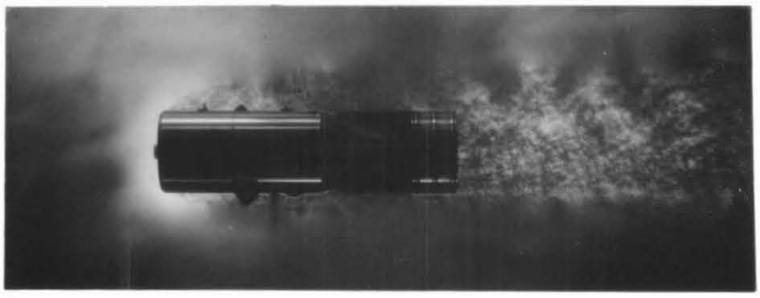

FIG. 8 – FLOW PATTERN AS OBSERVED WITH POLARIZED LIGHT

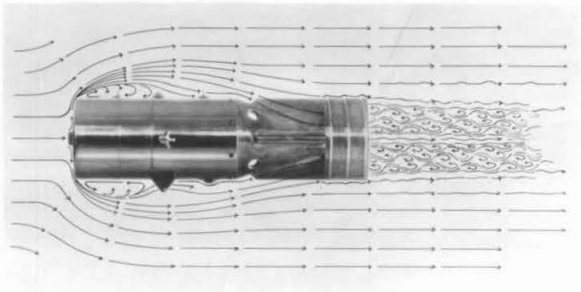

FIG. 9 – FLOW DIAGRAM AS CONSTRUCTED FROM OBSERVATIONS IN POLARIZED LIGHT FLUME

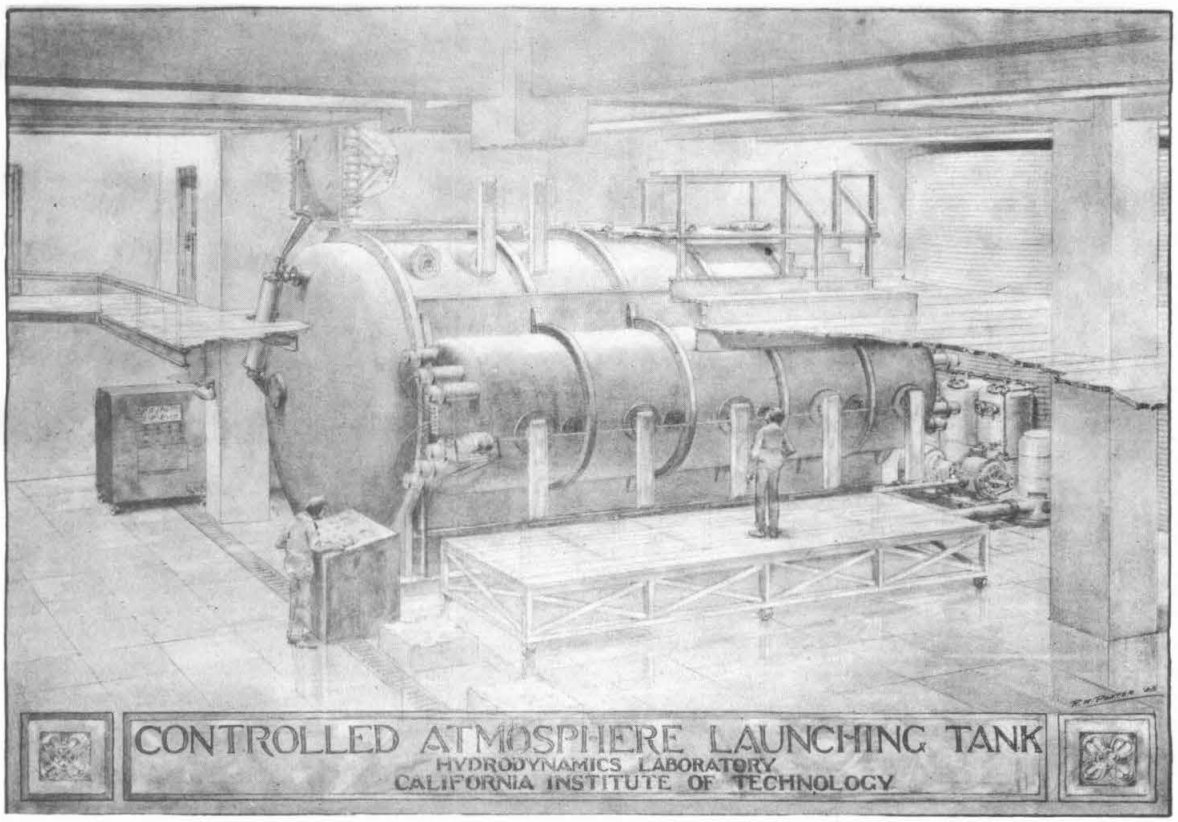

FIG. 10

CONTROLLED ATMOSPHERE LAUNCHING TANK

The controlled atmosphere launching tank was constructed for the specific purpose of investigating the hydrodynamic problems involved as the projectile enters the water from the air. It was decided to standardize upon the same size of models for this tank as for the High Speed Water Tunnel; namely, two inches in diameter. In using projectiles of this small size it is necessary, in order to simulate accurately the conditions existing in prototype launchings, to reduce the pressure of the air in accordance with the scale ratio used in constructing the projectile. Therefore, the launching tank is constructed as a pressure vessel to withstand an external pressure of one atmosphere. Figure 10 shows a perspective drawing of the equipment and serves to illustrate its method of operation. The equipment may be subdivided into four sections:

A. The tank itself, with its filter, storage, and air systems

B. The launcher

C. The observation cameras

D. The system of illumination

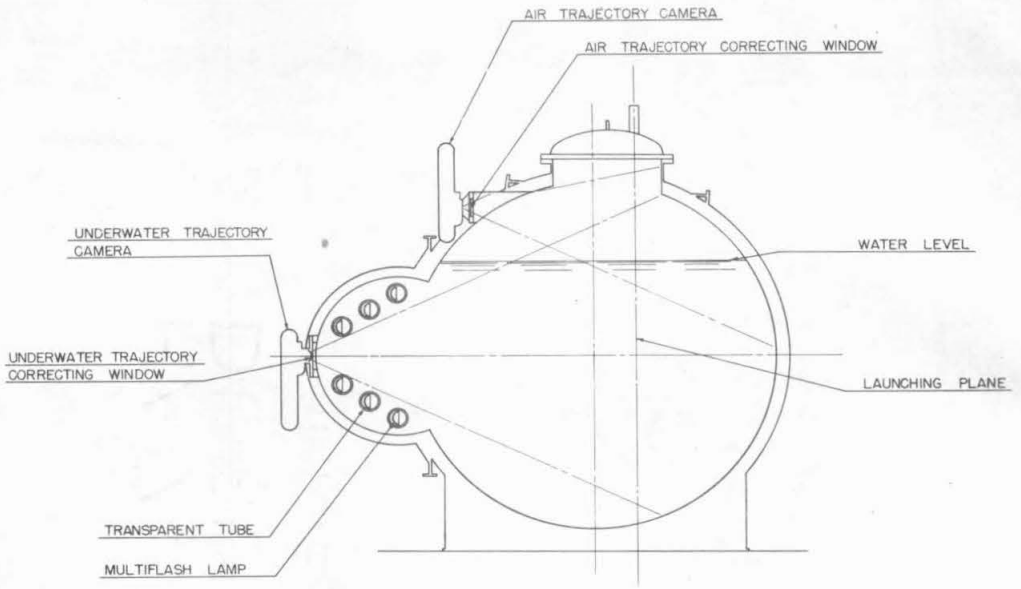

FIG. 11 – SECTIONAL VIEW OF INTERFACE TANK SHOWING CAMERA FIELDS

A. The Tank and Auxiliary Equipment

The tank itself is constructed from sections of 2 cylinders. The main cylinder is 13 feet in diameter and about 30 feet long, the auxiliary cylinder is welded to one side of this with its axis parallel to the main one. It is 6 feet in diameter and about 24 feet long. Figure 11 shows a cross section of the construction. The purpose of the auxiliary cylinder is to increase the distance between the plane of launching and the observation windows for the cameras. This increase is necessary to make it possible to cover the depth of the tank with the field of view of one camera. Since the purpose of the small cylinder was to provide observation windows for the cameras, it was necessary to put the minimum obstruction of the plane of intersection of the two cylinders. However, there is obviously a very great collapsing force on the tank when the pressure is reduced below atmosphere. In order to carry this collapsing load, heavy struts were installed in this plane midway between the camera stations. The load was carried from the shells to these struts by means of deep beams welded to the cylinders in the plane of the intersection. One of the by-products of designing the tank to withstand an external pressure of one atmosphere is that the tank is able to withstand an internal pressure considerably in excess of that amount. It has been tested up to about 60 pounds per square inch above atmosphere and is usable for experiments over three-quarters of this range.

Two large corrugated galvanized storage tanks were provided and connected to the launching tank through large pipes and a transfer pump so that the tank could be emptied or filled rapidly as the experimental work required. A small sand filter was provided to clarify the water used in this system to decrease as much as possible the amount of light absorbed by the water so as to permit the taking of high-speed motion pictures. A rotary "wet" type of vacuum pump was provided to control the pressure of the air above the water surface.

B. The Launcher

One of the limitations inherent in the operation of a variable pressure launching tank is that the size of the tank must be kept as small as possible in order to make its construction economically feasible. This means that the space available for the mechanism required to launch the model is very much more limited than that for a tank operated at atmospheric pressure. An analysis of the launching devices previously used in other laboratories showed that most of them required more space than could be made available and that the most common type, the "air gun," had the further objection that the amount of air released by it at each launching would be large enough to affect the atmospheric pressure within the tank. Consequently, it was decided to attempt the construction of a centrifugal type launcher since analysis showed that it could be built in a relatively small space and at the same time could be made to operate over a wide range of trajectory angles. Furthermore, no air is required for its operation, and thus the difficulty from this source is completely eliminated. Figure 12 shows two views of this launcher. It is constructed to hang from the underside of the main hatch cover located at one end of the launching tank. The hatch cover is hinged, and opened and closed by a hydraulic cylinder. When the cover is open, the launcher is completely accessible from the top of the tank for loading, setting, and maintenance purposes. The launcher is designed to project the model at any desired speed up to 250 feet per second. The trajectory angle can be set at any point between vertical and horizontal. In addition, the projectile can be launched with any desired angle of pitch with respect to the trajectory of between 10 degrees nose down and 10 degrees nose up. When ready for launching, the projectile is held tightly in a chuck on the launching wheel. Figure 13 is a sectional perspective drawing of this chuck. As the wheel revolves, the chuck and projectile are kept from rotating about the chuck axis by a train of gears which mesh with a stationary master gear concentric with the axis of the launching wheel. The projectile is held in the chuck by a single finger, which is kept in place by a sear and trigger. The position at which this trigger is tripped controls the trajcetory angle. The trigger is tripped by striking an adjustable stop which is carried on an arm that carries the quadrant and scale for the selection of the trajectory angle. This arm also carries the master gear of the chuck gear train. Rotation of the arm therefore rotates this master gear, and changes the angle

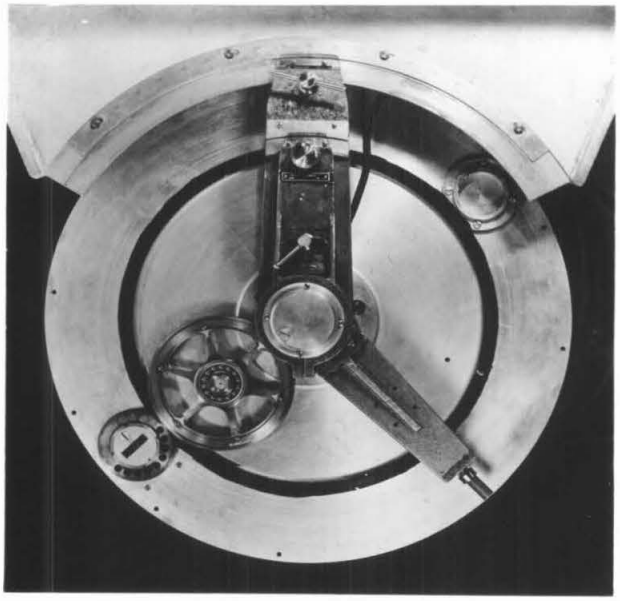

VIEW SHOWING GEARING, TRIPPER, AND ANGLE SETTING DEVICE

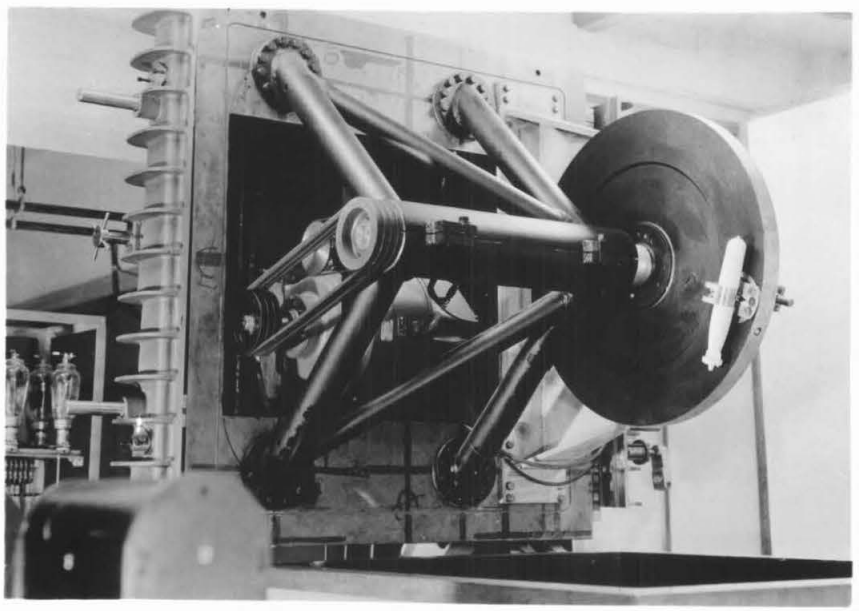

VIEW SHOWING MODEL IN CHUCK

FIG. 12 – CENTRIFUGAL MODEL LAUNCHER

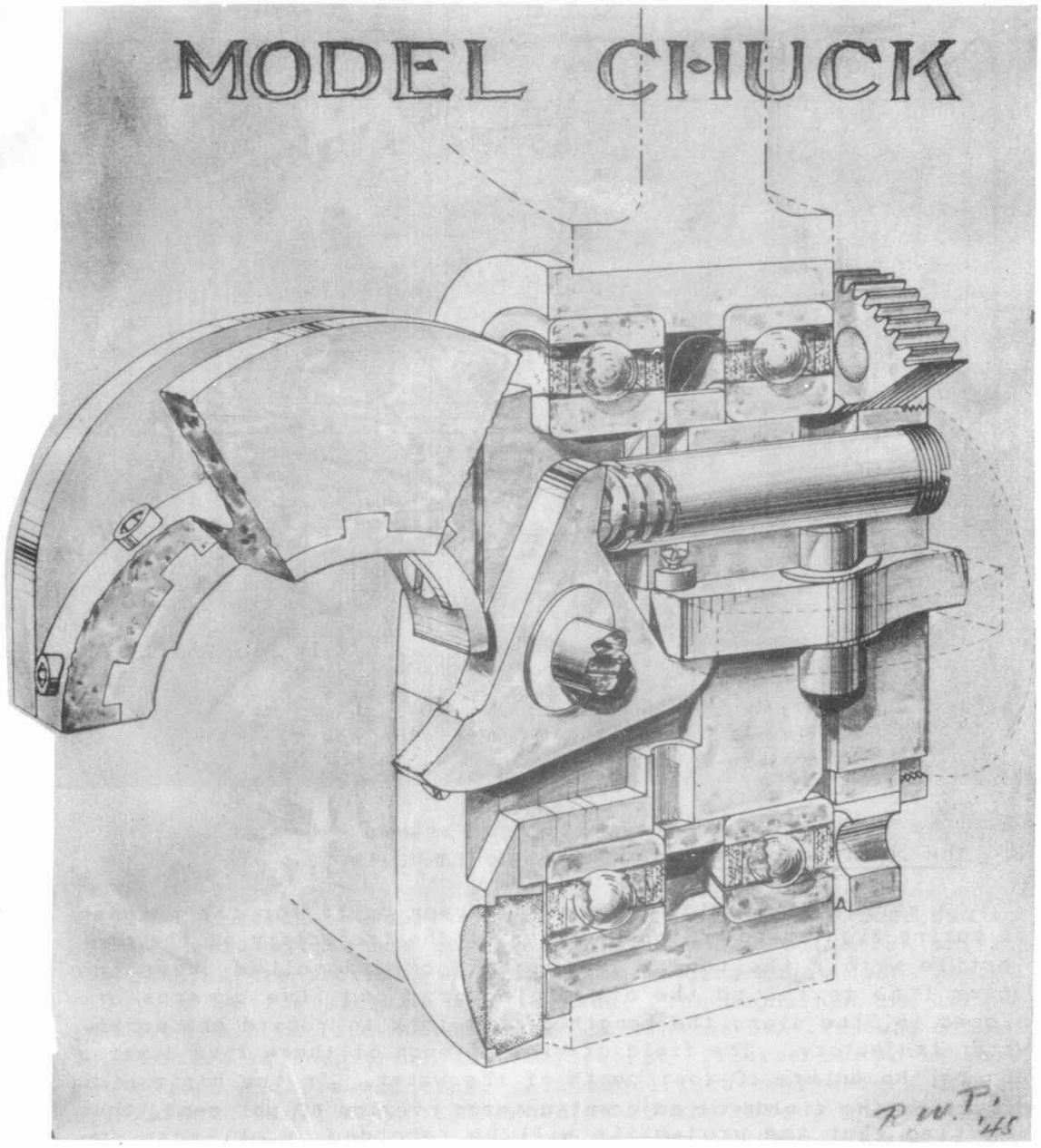

FIG. 13 – INTERNAL CONSTRUCTION OF MODEL CHUCK

of the projectile with the horizontal to correspond to that of the selected trajectory. The pitch angle is introduced by an additional adjustment between the master gear and the trip arm, which permits of the plus or minus 10 degree movement previously described. The characteristics of this launcher have been carefully measured. It has been determined that trajectory and pitch angles are both reproducible within plus or minus two-tenths of a degree of the set values. The speed of the projectile can be controlled as accurately as the speed of the rotating launcher can be measured, which is less than one foot per second.

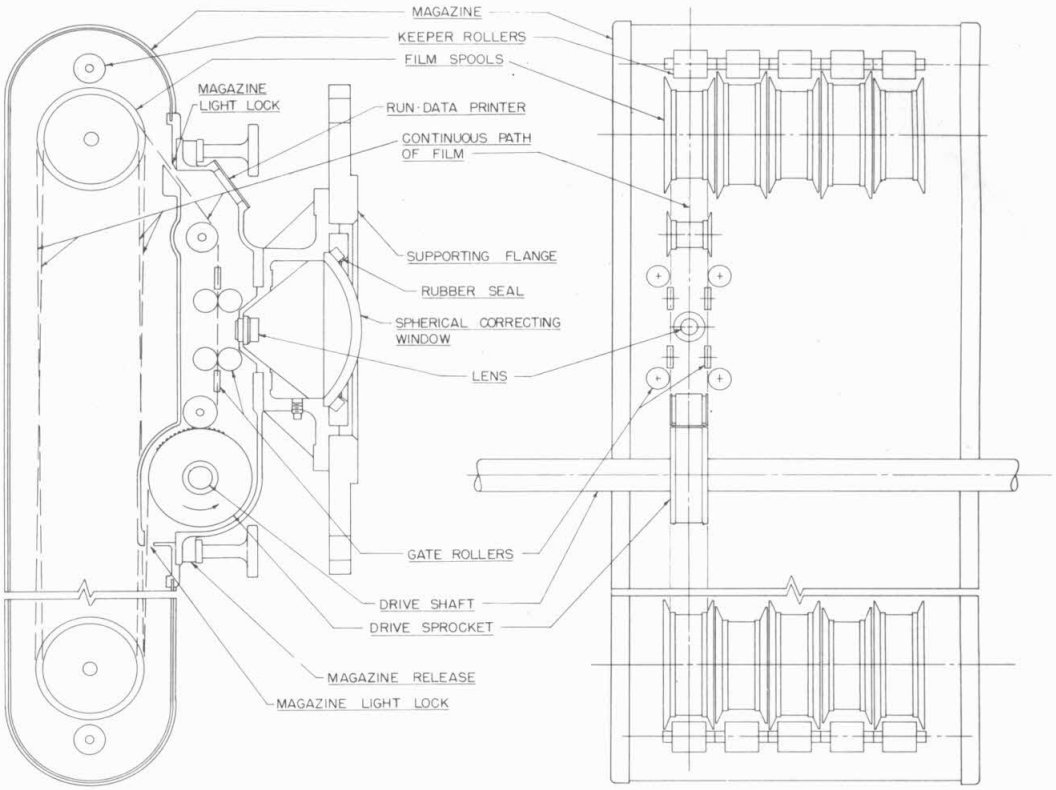

FIG. 14 — OUTLINE DRAWING OF CAMERA AND MAGAZINE

C. The Observation Cameras

A series of special cameras has been built for the purpose of taking high speed motion pictures of the trajectory of the projectile within the tank. Two cameras are installed above the water line to record the air trajectory, and five cameras are placed in line along the length of the tank to record the underwater trajectory. The field of view of each of these five cameras covers the entire 10-foot depth of the water. In the horizontal direction the fields of adjacent cameras overlap 60 per cent, thus insuring that the projectile will be recorded on at least two cameras at every point on its path. The purpose of this overlap is to make it possible to use stereoscopic means to determine orientation and position in space of the projectile at any time. The tank windows for the two air cameras are of optical glass with plane surfaces. The windows for the five subsurface cameras are ground spherical, and the camera lenses are accurately placed so that the nodal point of the lens comes at the center of curvature of the window. The result is that a picture without additional distortion is secured and the field of view is the same as for the lens in air. This construction reduces the number of cameras required to cover the launching plane from 12 or 15 to five.

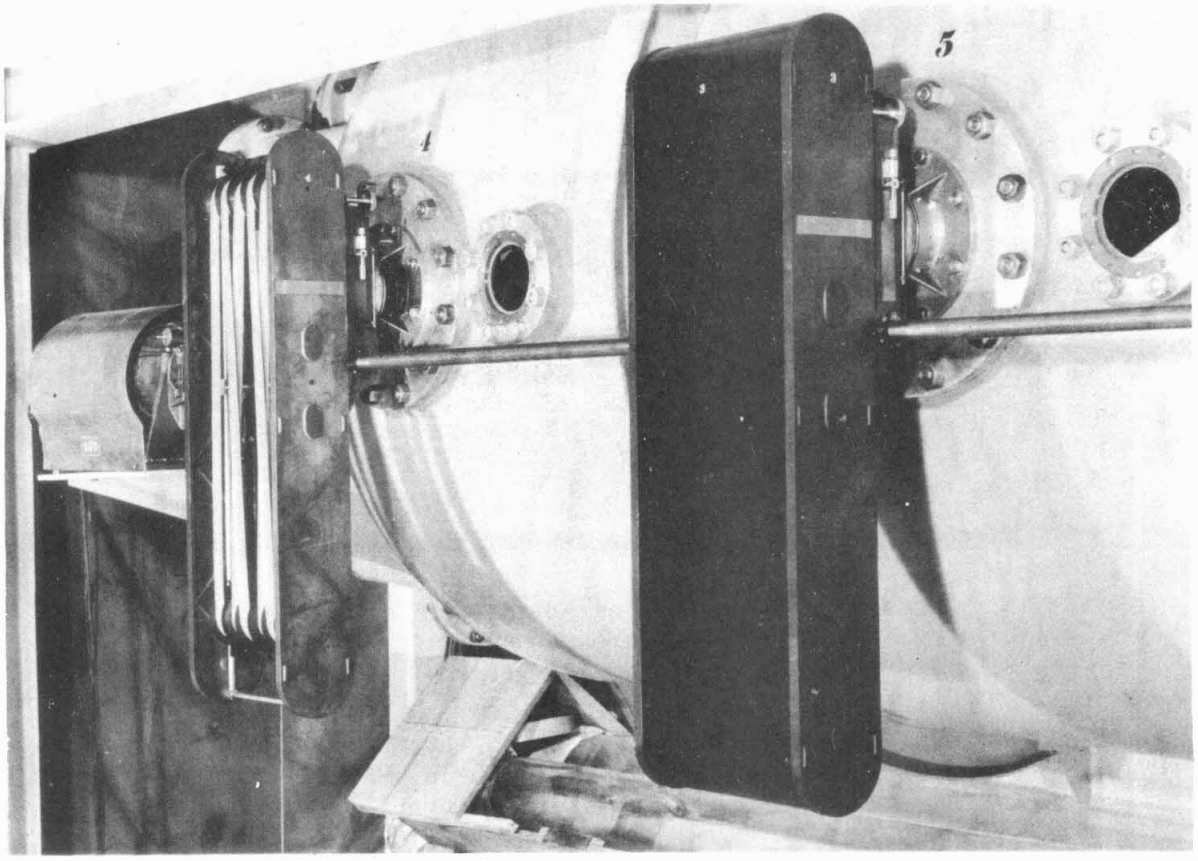

FIG. 15 – CAMERA AND MAGAZINE INSTALLATION SHOWING METHOD OF FILM LACING

The cameras themselves have no shutters and are designed to operate only with short duration multiflash illumination units. The cameras are provided with daylight loading magazines. Standard 35 mm motion picture film is used. The magazines are unique in that the film is cemented into a continuous belt instead of being carried on supply and take-up spools. Figures 14 and 15 show the camera and its magazine. All subsurface cameras are driven by a single shaft directly connected to the motor, whereas, the air-flight cameras are operated by Selsyns. Figure 16 shows the line of underwater cameras and the motor drive. The magazines hold enough film for a one-second exposure, which is the maximum time that will be required for any projectile to traverse the length of the tank. The film is operated at a speed of about 35 feet per second. In order to start and stop the film gradually so as to prevent tearing and at the same time permit the use of a synchronous motor to secure an exact predetermined speed, a special mounting has been designed for the camera drive motor. The entire motor frame is mounted on bearings concentric with the shaft. Slip rings are provided on the frame to carry the current to the motor when it is in any position - either stationary or rotating. Two brakes are provided, one on the shaft, and one on the stator, or frame. When the cameras are to be started, the shaft brake is locked to prevent rotation and the stator brake is

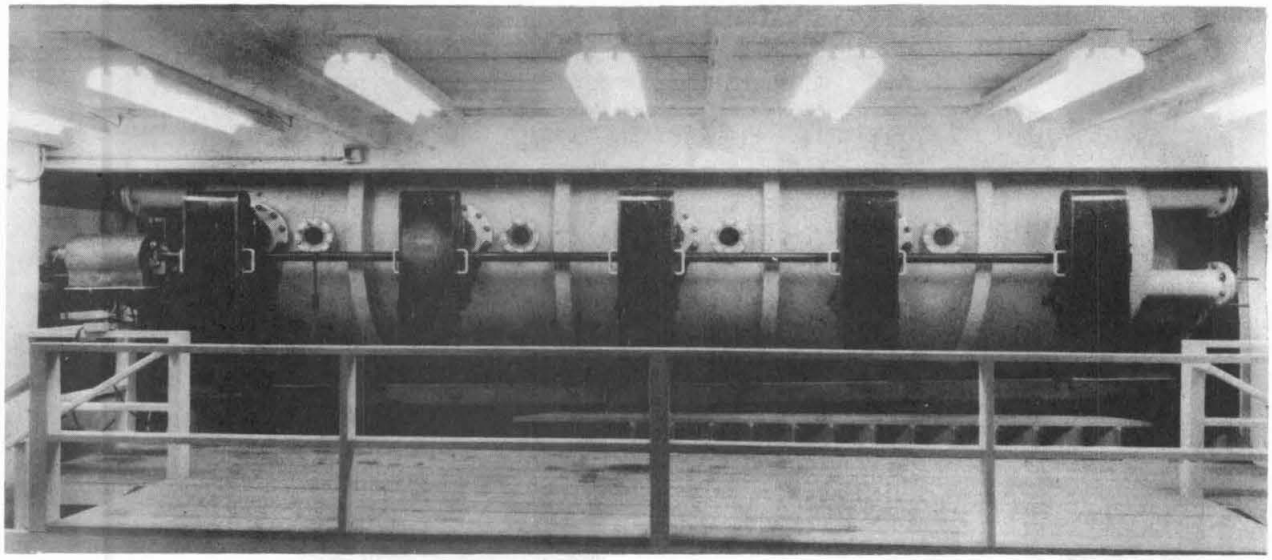

FIG. 16 – BATTERY OF SUBSURFACE CAMERAS AND MOTOR DRIVE

left free. The current is then applied to the motor and the stator revolves, coming up to synchronous speed in a few seconds. The shaft brake is then released and the stator brake is applied gradually through a torque-limiting mechanism until all the cameras together with their film are brought up to speed. Under operating conditions the stator brake is locked so that the cameras are all operated at synchronous speed. Smooth and gradual stopping at the end of the run is secured by going through this procedure in the reverse order.

D. The System of Illumination

The illumination system in the launching tank serves a dual purpose: that of providing the necessary light to take the picture and also of acting as a shutter for the camera. The illumination is provided by a series of synchronized high voltage flash lamps, each one operated by an individual control circuit. These units were designed and built under the supervision of Professor Harold Edgerton, of the Massachusetts Institute of Technology, and his associates.

The measurements have shown that the effective duration of the flash in these lamps is between one and two microseconds and that the individual units are synchronized within approximately one-tenth of a microsecond. They are capable of being operated at any desired speed up to 3000 flashes per second. Operating at this speed, the battery of lamps will require a continuous input of more that 100 kilowatts. Since the actual period of illumination is only of the order of 1/300 of the total time, the instantaneous rate of energy input during the illumination is about

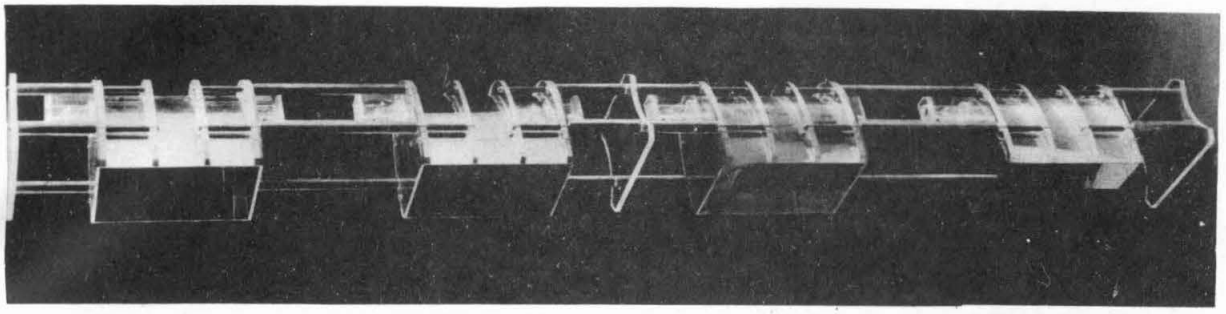

FIG. 17 – BANK OF HIGH SPEED FLASH LAMPS
MOUNTED IN THE ALUMINUMIZED LUCITE REFLECTORS

30,000 kilowatts. The flash lamps themselves are small diameter, straight, quartz tubes. They are mounted on special lucite reflectors designed and constructed in the laboratory. The inner surfaces of these reflectors are aluminumized. Figure 17 shows the appearance of a bank of these lamps mounted in their reflectors. In order to secure satisfactory record films from the launchings, a complete synchronizing control system has been worked out involving the launcher, the camera, and the lights. This insures that the cameras are running at operating speed at the instant of launching, that the launching takes place only just after the exposed "loading" strip of film has passed through the camera, and that the flash lamps are turned on a few frames before the launcher is tripped.

FREE SURFACE WATER TUNNEL

The free surface water tunnel was designed to make it possible to study the behavior of the projectiles under two sets of conditions which are difficult to work with in the High Speed Water Tunnel. The first is the behavior of underwater projectiles, such as torpedoes, when they are operating so close to the surface that the flow loses its symmetry. This region may be extended to include entrance phenomenon insofar as useful information concerning this transient state can be obtained from measurements made of the steady state conditions. The second condition is the effect of jet propulsion on underwater projectiles. This involves the injection of comparatively large volumes of air or other gas into the flow circuit. Special provisions are required for the removal of this gas, since if it is allowed to remain in the circuit, it not only obscures any visual observations, but modifies the forces on the projectile and alters the flow itself.

This water tunnel will have a working section 20 inches square and about 9 feet long. To secure maximum visibility, the walls are constructed of heavy lucite sheets. The thickness of this lucite is made sufficient to withstand an external pressure of one atmosphere, since it is planned to use the vacuum pump of

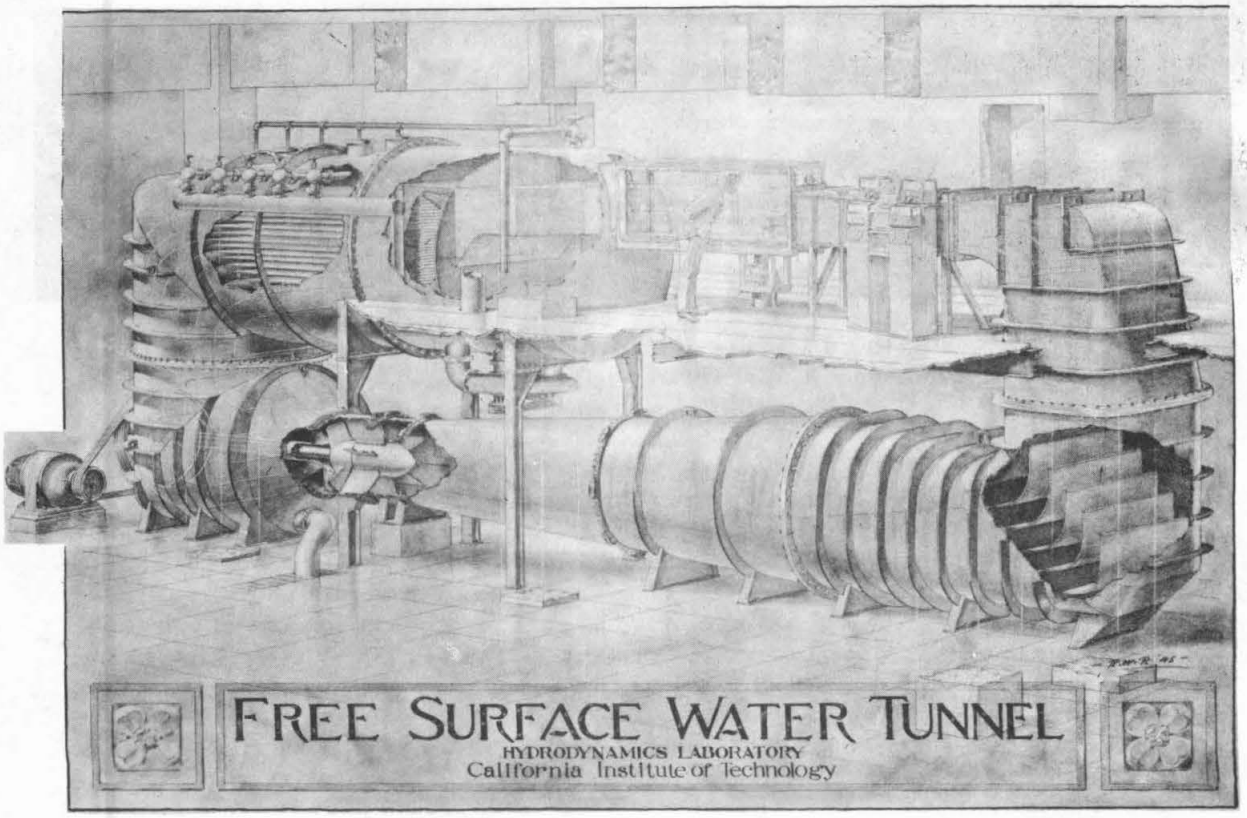

FIG. 18

the interface tank to control the atmospheric pressure above the free surface when making measurements of a type that will be affected by both the air and the water. The tunnel is designed to operate at a maximum velocity of 25 feet per second. The circulation is produced by a propeller pump of similar design to that employed in the High Speed Water Tunnel. The power requirements are much less, however, due to the lower velocities. The drive motor is 75 hp, which is less than 1/3 of the horsepower input at maximum velocity to the High Speed Water Tunnel. Figure 18 is a perspective drawing showing the general construction of this tunnel and the various features incorporated in it. It will be noted that just downstream from the working section, the flow passes through a series of diffuser vanes which decreases the velocity to about 1/16 of that in the working section. These vanes are followed by the gas separator section.

SUMMARY OF THE WORK OF THE LABORATORY

1. SPECIFIC INVESTIGATIONS

Appendix 1 contains a complete list of the reports issued by the Laboratory during the period of operation of the contract. The titles in the list indicate the range of problems studied during this time. It will be observed that there are 60 reports in the list. Since the duration of the project has been 46-1/2 months, this means that on the average a problem has been completed and reported every 24 days, including the time for initial design and construction. It is very difficult for the project staff to evaluate the usefulness of the results obtained in the Laboratory. In general, the reports have been completed and distributed to the organizations within the Army and Navy that have interests in such problems. With such a varied distribution, it is only by chance that the Laboratory learns of any use that has been made of its results. However, a few comments can be made on the basis of this chance information.

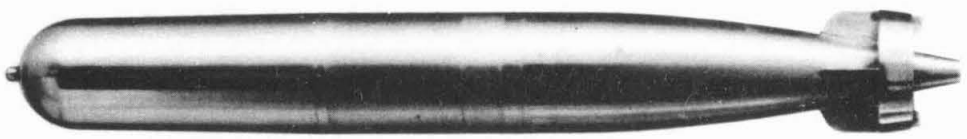

FIG. 19 – MODEL OF MK 13 TORPEDO WITH SHROUD RING

a. Shroud Ring

One of the clearest cases of known application of the Laboratory results was the development of the shroud ring for the Mark 13 Aircraft Torpedo. The use of the shroud ring was proposed by the Laboratory September 4, 1943. Its original purpose was primarily to increase the stability during the steady state operation, but it was also felt that it might result in improvement of the performance during the entry phase. Tests were made in the High Speed Water Tunnel and in the Polarized Light Flume to determine the best dimension, location, and cone angle for the shroud ring. Its effects on the rudders and elevators were investigated, as well as the effect on the stability. As a result of these measurements, the Laboratory selected a given set of specifications as being the most promising ones for trial. Full-scale launching tests were first made in the torpedo launching tube at Morris Dam, operated under Contract OEMsr-418 at the California Institute of Technology. These tests indicated a substantial improvement in the entry characteristics of the torpedo when fitted with a shroud ring. The tests were followed by field tests with airplane drops made by the Navy at San Diego and later repeated at the Torpedo Station at newport, Rhode Island. Service tests were then carried out and as a result, the shroud ring was adopted as standard equipment for the Mark 13 Torpedo. Figure 19 shows a photograph, taken in November, 1943, of the 2-inch model of the Mark 13 complete with shroud ring as recommended by the Laboratory. This work was presented in Reports Section Nos. 6.1-sr207-939 and -1905.

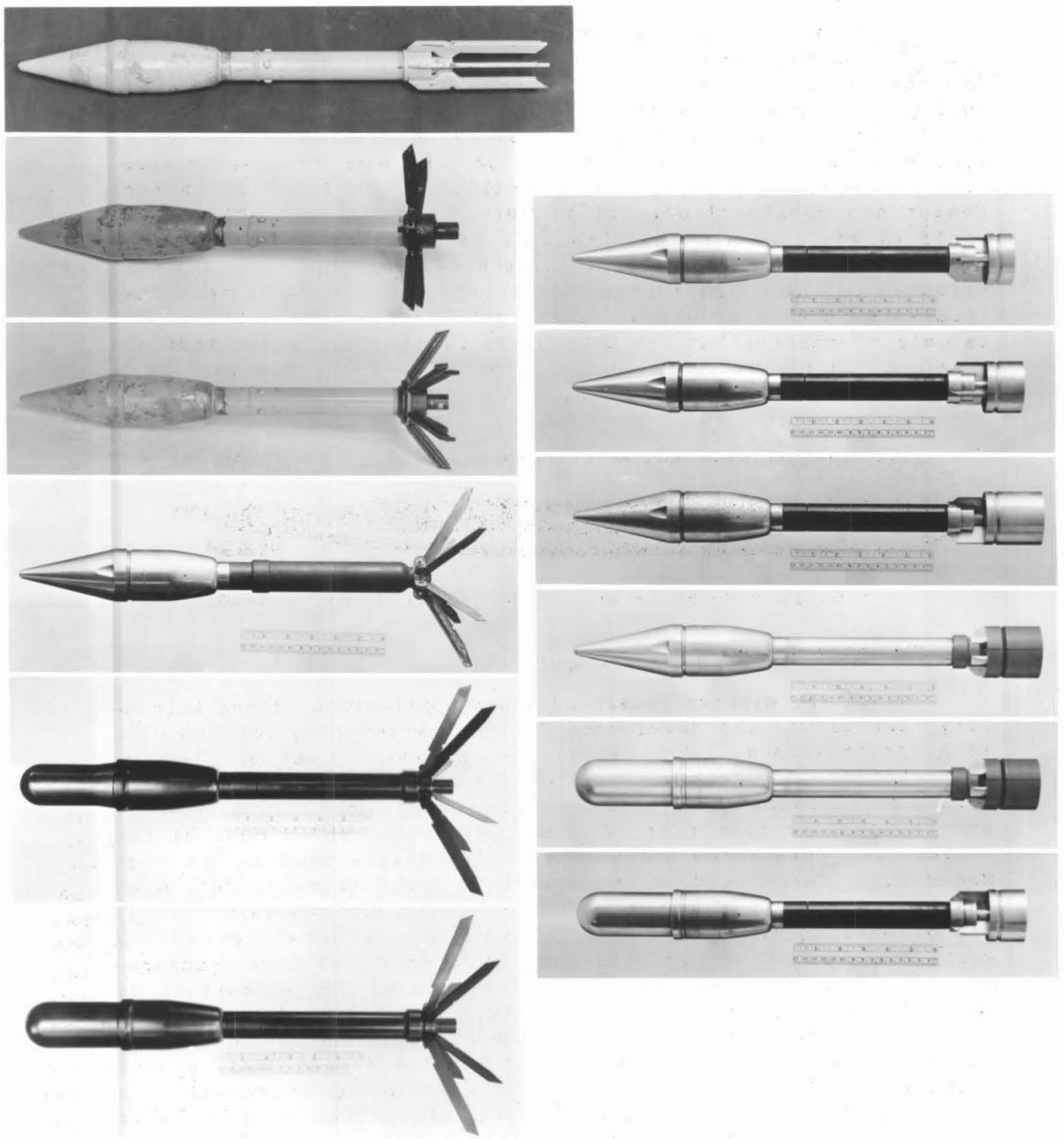

FIG. 20 — GROUP OF MODELS OF THE BAZOOKA

b. Bazooka

Shortly after the Bazooka was first used in the field, it was felt that the accuracy was not completely satisfactory and that it could be improved by increasing the stability of the projectile. Extensive studies were carried on in the Water Tunnel which led to the development of a ring tail which proved to be satisfactory and was adopted for use on the early models. Tests were also made of subsequent modifications of the explosive head and helped to select the shapes with the most satisfactory performance. The results of these studies were presented in Reports Section Nos. 6.1-sr207-1314, -1303, -276, -920, and -934. Figure 20 shows a group of the Bazooka models.

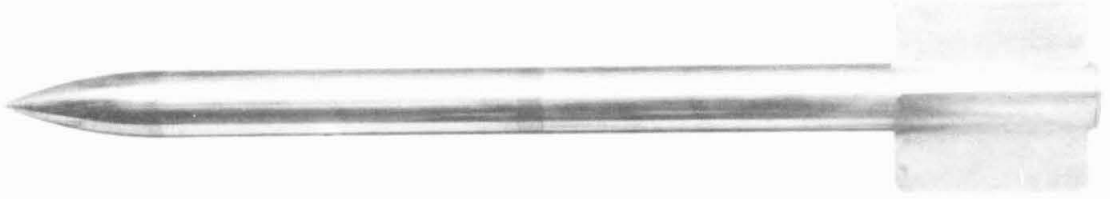

FIG. 21 – MODEL OF 2-1/4" ANTIAIRCRAFT ROCKET

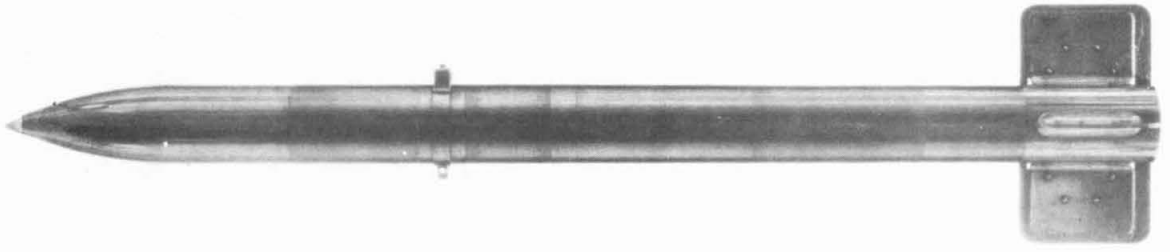

FIG. 22 – MODEL OF 5" HIGH VELOCITY AIRCRAFT ROCKET

c. Other Rockets

Detailed studies were made of several other rockets which led to changes in designs which were incorporated in the production units with resulting improvements in their performance and effectiveness. The 2-1/4-inch AA Rocket, the 5-inch HVAR Rocket, the Army 4-5-inch Rocket, the 3-5-inch and 5-inch Spin Stabilized Rockets, and the 7.2-inch Chemical Rocket belong in this class. Reports ND-13, Section Nos. 6.1-sr207-927, -2241, -1312, -1304, -1919, -1270, -1903, -2239, -1261, and -932 present the results obtained in the Water Tunnel. Figure 21 shows the model of the 2-1/4-inch AA Rocket, Figure 22 the 5-inch HVAR Rocket, Figure 23 the 4.5-inch Rocket, Figure 24 the 3.5-inch SSR, and Figure 25 the 7.2-inch Chemical Rocket.

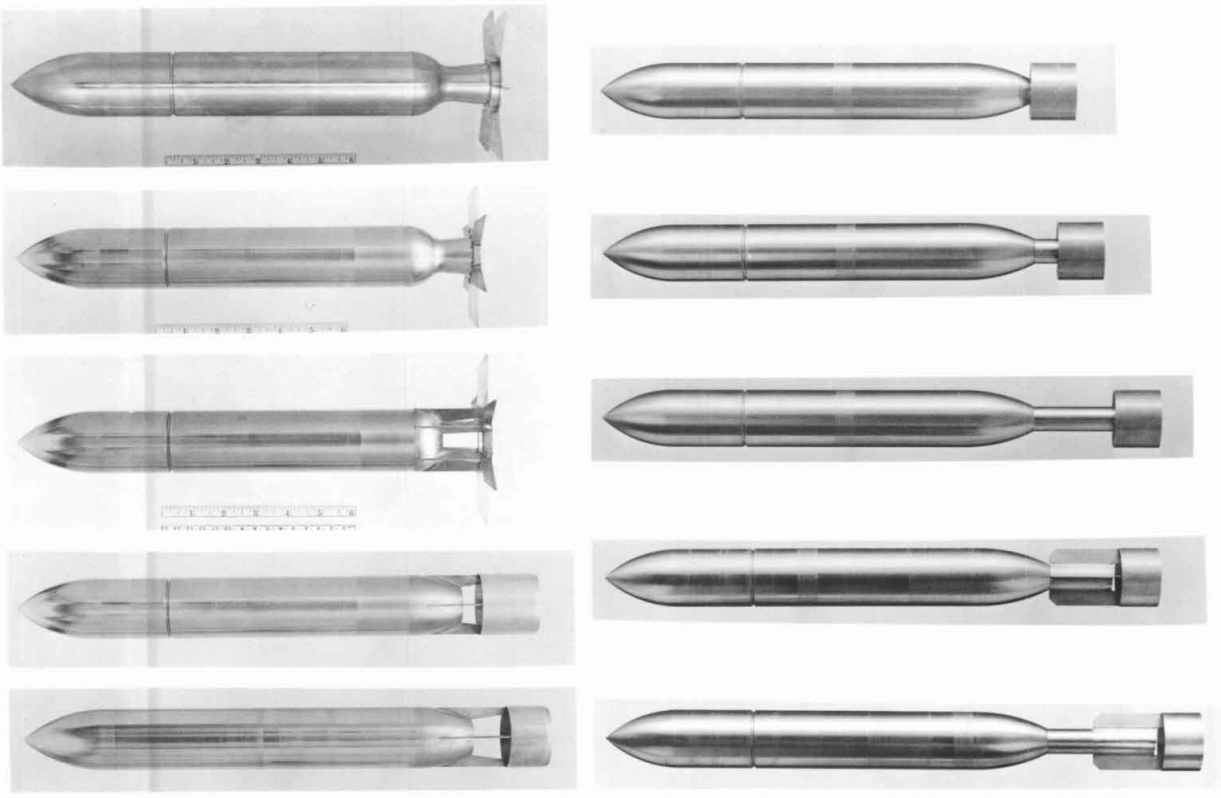

FIG. 23 – GROUP OF MODELS OF 4-1/2" ROCKET

FIG. 24 – MODELS OF THE 3-1/2" SPIN-STABILIZED ROCKET

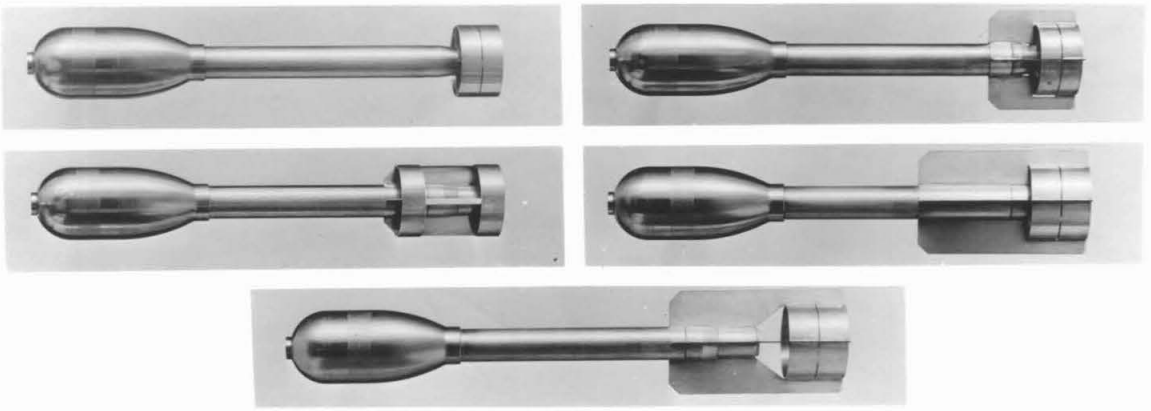

FIG. 25 – MODELS OF 7.2" CHEMICAL ROCKET

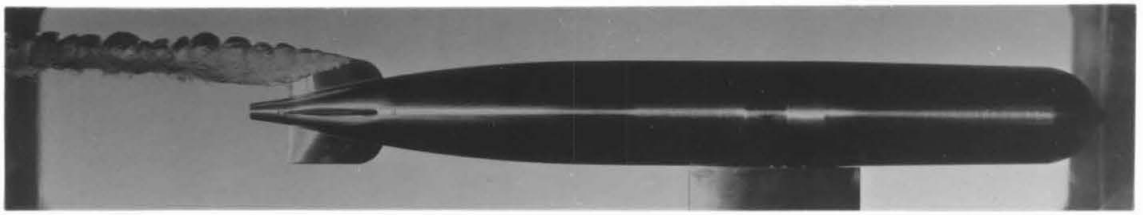

FIG. 26 – MODEL OF MK 25 TORPEDO WITH EXHAUST FROM UPPER FIN

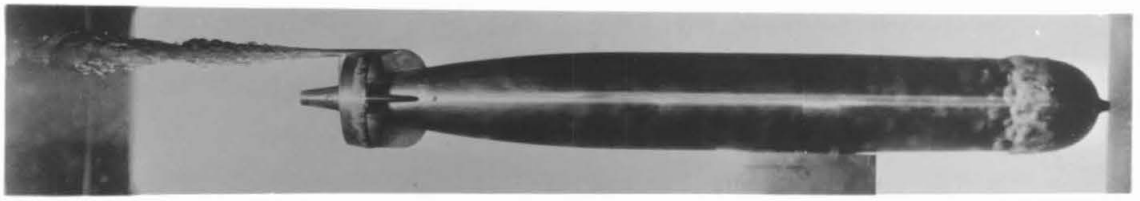

FIG. 27 – MODEL OF MK 25 TORPEDO WITH SINGLE HORIZONTAL EXHAUST PIPE

d. Mark 25 Torpedo

In the development of the Mark 25 Aircraft Torpedo, the designers wished to avoid the use of the hollow propeller shaft as the exhaust pipe for the turbine gases. It was originally proposed that those gases should be discharged from the tip of the upper fixed fin. This possibility was investigated by the Laboratory and found to be quite unacceptable because of its effect on the propellers and control surfaces. A substitute method was proposed and investigated, which used short exhaust stacks projecting back from the rear edge of the shroud ring.

FIG. 28 – MODEL OF MK 25 SHOWING TWIN EXPANDING EXAUST PIPES

The locations and minimum lengths of satisfactory stacks were determined by the Laboratory and these stacks were incorporated in the final design. Five reports, Section Nos. 6.1-sr207-1275, -1640, -1642, -1916, and -2236 cover this work. Figure 26 shows the Mark 25 model under test in the tunnel with the unsatisfactory exhaust port in the top fin, Figure 27 the first design of a horizontal exhaust pipe, and Figure 28 the twin exhaust pipes finally recommended.

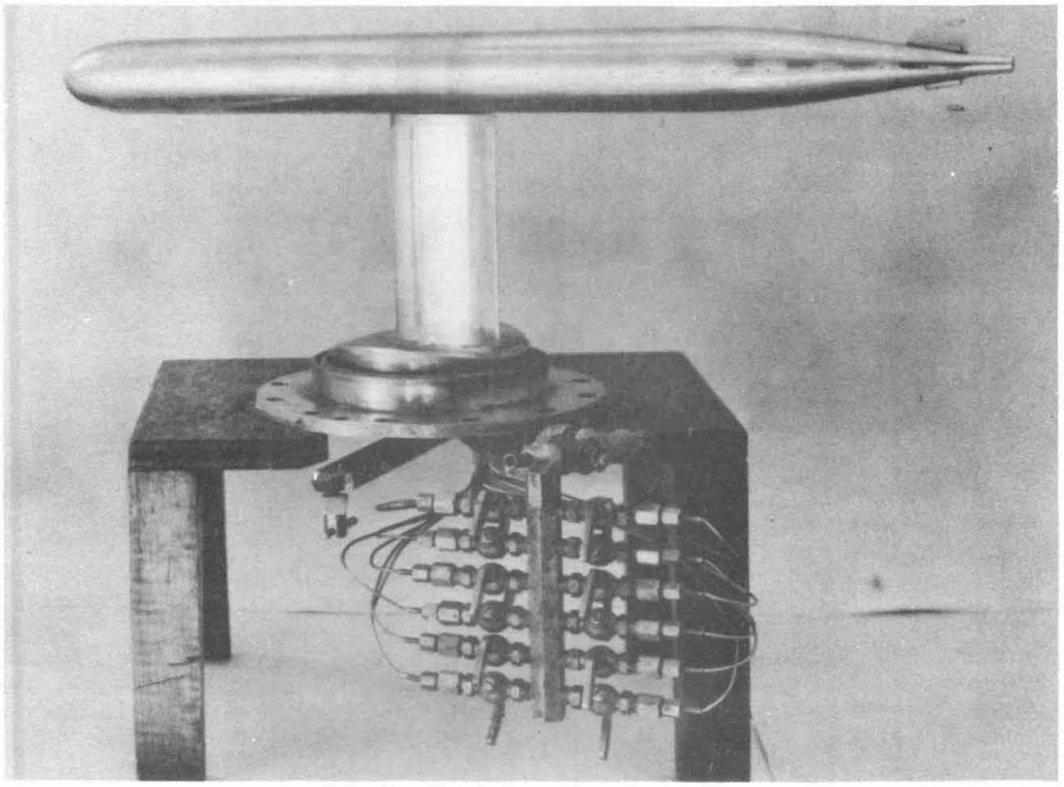

FIG. 29 – MODEL OF MK 14 PRESSURE DISTRIBUTION MODEL MOUNTED FOR INSTALLATION IN TUNNEL

e. Pressure Distribution Tests

One class of measurements that has proved useful has been the pressure distribution tests on the various torpedo shapes. Such tests have been made on the Mark 13, 14, 15, and 25. The information obtained has been useful in the development of exploder mechanisms as well as in the depth control mechanisms for the torpedoes. This work has been presented in Reports Section Nos. 6.1-sr207-1643, -1905, -2244, and -2248. Figure 29 shows the model of the Mark 14 mounted on the pressure distribution shield, ready for installation in the Water Tunnel.

2. GENERAL INVESTIGATIONS AND DEVELOPMENTS

During the life of the contract, the main objective of the work of the Laboratory has been the solution of specific problems directly related to service projectiles and equipment. Due to the urgency of this class of work, little time has been available for general studies in the field of exterior ballistics. However, during the last year of the contract, it has become possible to integrate series of specific investigations to a sufficient extent to formulate some general conclusions in several subfields. Whenever time would permit, summaries of material of this character have been prepared and presented in the forms of reports. The following paragraphs contain a brief review of some of the more important aspects of these general investigations:

a. Use of Stabilizing Surfaces on Nonrotating Rocket Projectiles

In the course of the rocket program carried out at the California Institute of Technology under Contract OEMsr-418, one general type of design developed which was used for many applications consisted of a pointed or ogival nose on a cylindrical body which was cut off square at the after end. Stabilizing surfaces consisted of four radial fins attached to the after end of the cylinder. Rockets of this type were made of many diameters and ratios of overall length and diameter. In order to assist in the design of new adaptations, a systematic series of tests was carried out, using the 5-inch HVAR body, to determine the effect of various proportions of these fins, the effect of moving them forward or aft, and the effect of increasing their radial width. Furthermore, a second systematic series of measurements was carried out with comparable variables to determine the stabilizing effect of ring or drum tails carried on the outer diameter

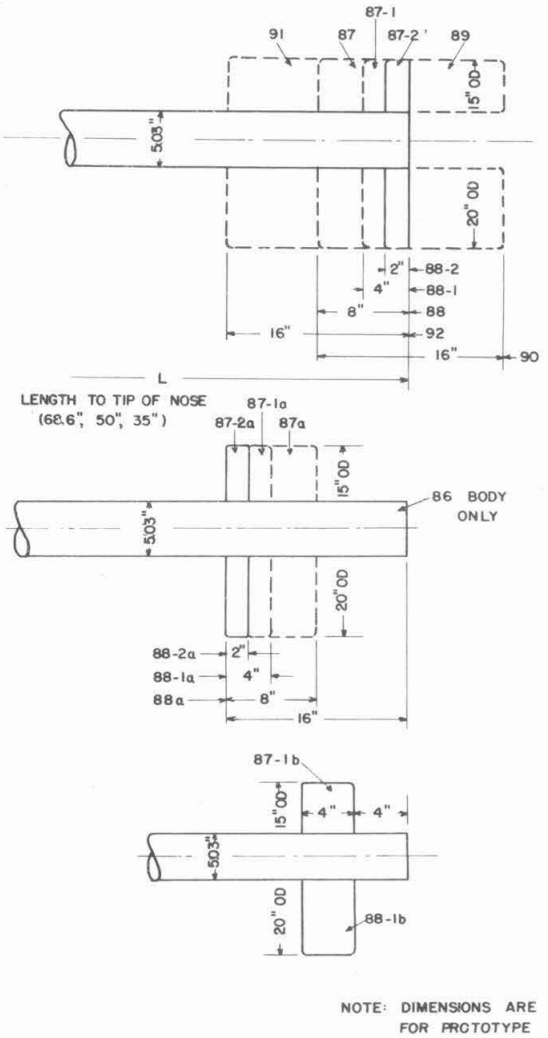

NOTE: DIMENSIONS ARE FOR PROTOTYPE

FIG. 30 – RELATIVE DIMENSIONS OF FIN SETS

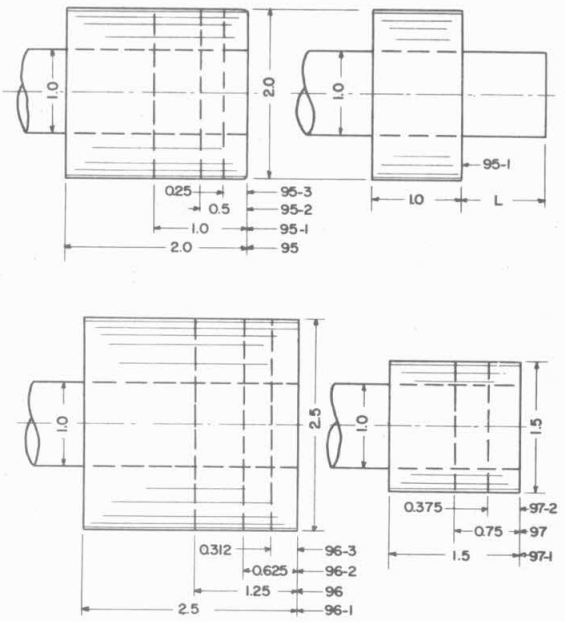

FIG. 31 – RELATIVE DIMENSIONS OF RING TAILS

of the four fixed vanes. The results of these tests were presented in Report Section No. 6.1-sr207-2241 (5-inch HVAR). Figure 22 shows a photograph of the basic model, Figure 30 is a drawing showing the dimensions of the various sets of fins tested, and Figure 31 the corresponding detail of the group of ring tails investigated.

The conclusions may be summarized briefly as follows:

1. The ring tail is far more effective in producing stability than the fin-type tail when physical dimensions alone are considered.

2. The stabilizing moment increases very rapidly, with an increase in the outside diameter of either the fin or the ring tail. This is due primarily to the greater amount of fluid whose motion is affected by the larger surfaces, but it also results in part from the decrease in the relative effect of body interference and, in the case of the fins, the tip losses.

3. Very little, if any, increase in stability results from an increase in axial length of fins beyond a length of 2/3 the fin diameter.

4. The critical length of ring beyond which little increase in stability takes place lies between 1/2 and 2/3 the ring diameter.

5. For a given fin or ring tail, and for small angles of yaw, the restoring moment, measured around a center of gravity located at a constant percentage of the projectile length aft of the nose, varies directly with the overall length between about 7 and 14 calibers. In other words, in this range of lengths, the moment coefficient is constant.

b. Effect of Projectile Components on Characteristics of Overall Projectile

Measurements were taken on nearly all of the projectiles studied to determine their drag and cross force. A comparative study of the results of many of these tests showed that although

it is perfectly true that each major component of the projectile may modify the entire flow picture, nevertheless it is possible to draw at least some semiquantitative conclusions regarding the effect of each component going to make up the projectile upon the performance of the projectile as a whole. The word, "component" is taken to mean a major division of the projectile such as nose, body or center section, afterbody, tail structure. Consequently an analysis was made of the material available, together with a few additional tests to clarify special points. Although many of the findings of this analysis were merely confirmations of knowledge previously available in the field of aerodynamics of airships, they are not commonly recognized in the field of projectile designs. A few of these findings may be summarized as follows:

1. A blunt shape used as a nose may increase the drag of a projectile more than will the same shape used as an afterbody. An example of this is shown in Figure 32.

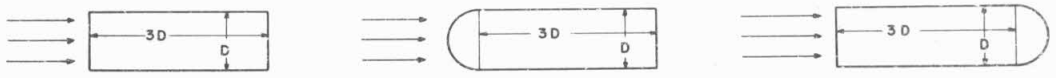

$C_D = 0.880$ $C_D = 0.273$ $C_D = 0.818$

FIG. 32 – RELATIVE DRAG COEFFICIENTS OF SIMPLE BODY SHAPES

2. If nose and other main components of a projectile are poor, minor projections such as fuzes, supporting lugs, bourrelets, etc., will have little effect on the overall drag. If the projectile is well streamlined, the same minor projections will cause an appreciable increase in drag. Figure 33 illustrates this effect as observed on tests of the AN Mark 41 Bomb. It will be noted that for the original bomb with the blunt nose the drag coefficient was unchanged by the removal of the lugs and projections. When a less blunt nose was used, the drag coefficient was lessened, but it was reduced an additional 10 per cent by the removal of the same lugs and projections.

3. Reductions in drag coefficients measured on models on which "fine" noses are substituted for hemispherical or blunter ones, may not be entirely realized on the prototype when similar changes are made. The reason is that the rate of decrease of drag coefficient with increase in Reynolds number is less for fine noses than for blunt ones.

4. The major factors determining the cross force on a projectile are the shapes of the nose, afterbody, and tail.

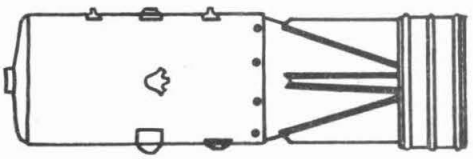

MK 41 BOMB

C_D = 0.61

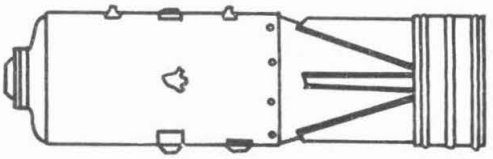

NOSE NO. 2 ON MK 41 BOMB

C_D = 0.355

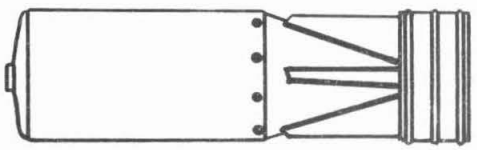

MK 41 BOMB
WITH SUSPENSION FITTINGS REMOVED

C_D = 0.61

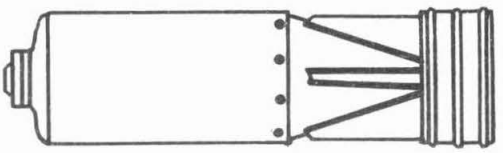

NOSE NO. 2 ON MK 41 BOMB
WITH SUSPENSION FITTINGS REMOVED

C_D = 0.32

FIG. 33 – EFFECT OF MINOR PROJECTIONS ON OVERALL DRAG

5. The major factors determining the moment on a projectile are the shapes of the nose, afterbody, and tail and the distance of these components from the center of gravity. Thus, since the moment coefficient is proportional to the moment divided by the length, it varies very little if at all with changes in length of the projectile, so long as the nose, afterbody, and tail shapes are not changed.

6. Tail surfaces form a relatively large fraction of the total wetted surface of a projectile and therefore contribute a significant factor of the skin friction drag. The area of the front edges of the tail fins is an appreciable part of the total frontal area. Unless they are carefully shaped, they will have a high drag per unit of area and thus will increase the overall drag coefficient a disproportionate amount.

7. Tail surfaces, to be effective, must be located so that high velocity flow passes over their entire area. If the flow is blocked away from these surfaces, the effectiveness of the tail is destroyed or reduced.

c. Forces on Finless Body Shapes

In an effort to understand more completely the problem of stability of projectiles and the effect of stabilizing surfaces, data have been collected on the cross force and moments of finless body shapes suitable for use on stabilized projectiles. Such body shapes are basically unstable and are only brought into the stable range by the addition of suitable stabilizing surfaces,

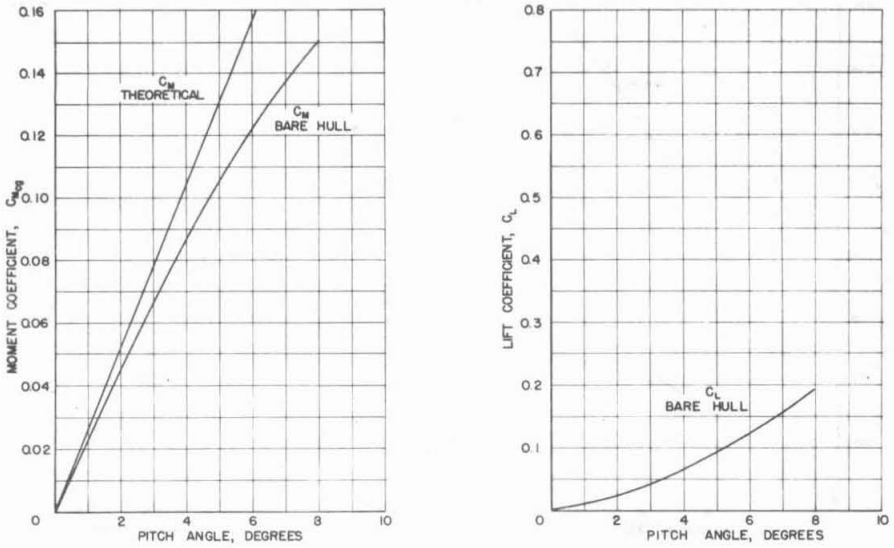

FIG. 34 - LIFT AND MOMENT COEFFICIENTS FOR BARE HULL OF MK 14-1 TORPEDO

such as fins and ring tails or by the use of spin. However, bodies of different shapes have differing degrees of instability, as may be seen from the following brief summary of the results:

1. Theoretical calculations show that a streamlined finless body moving in a perfect fluid should experience no cross force, but should have a rather large destabilizing moment. However, the movement of such a body in a real fluid results in a cross force as well as a moment. This cross force is the result of vortices forming at the after end of the body, therefore its line of action is near the tail, and its effect is to produce a stabilizing moment component which lessens the destabilizing moment caused by the overall flow pattern. Figure 34 shows this effect with results from tests on the Mark 14-1 Torpedo body.

2. Projectiles with blunt afterbodies have higher cross force coefficients than do streamlined projectiles. For this reason the destabilizing moment coefficient is less for the blunt than for the streamlined projectile. Figure 35 shows such a comparison between a finless Mark 14 Torpedo body and 5-inch SSR Rocket.

3. The effect of a unit of body cross force in reducing the destabilizing moment appears to be greater for the blunt afterbody than for the streamlined one. Apparently the line of action of the cross force is nearer the tip end of the blunt body.

4. For very small yaws, projectiles with blunt afterbodies may have a stabilizing moment of very low magnitude. This region is apparently affected by the nose shape as well as by that of the afterbody, and may be due to the effect of the nose shape on the drag.

on many different shapes. In order to assist the projectile designer in visualizing the possible flow pattern on new projectiles, these flow diagrams have been presented in a group of systematic series of projectile components. This collection was presented in Report Section No. 6.1-sr207-1649. A few typical diagrams are shown in Figures 38 to 40.

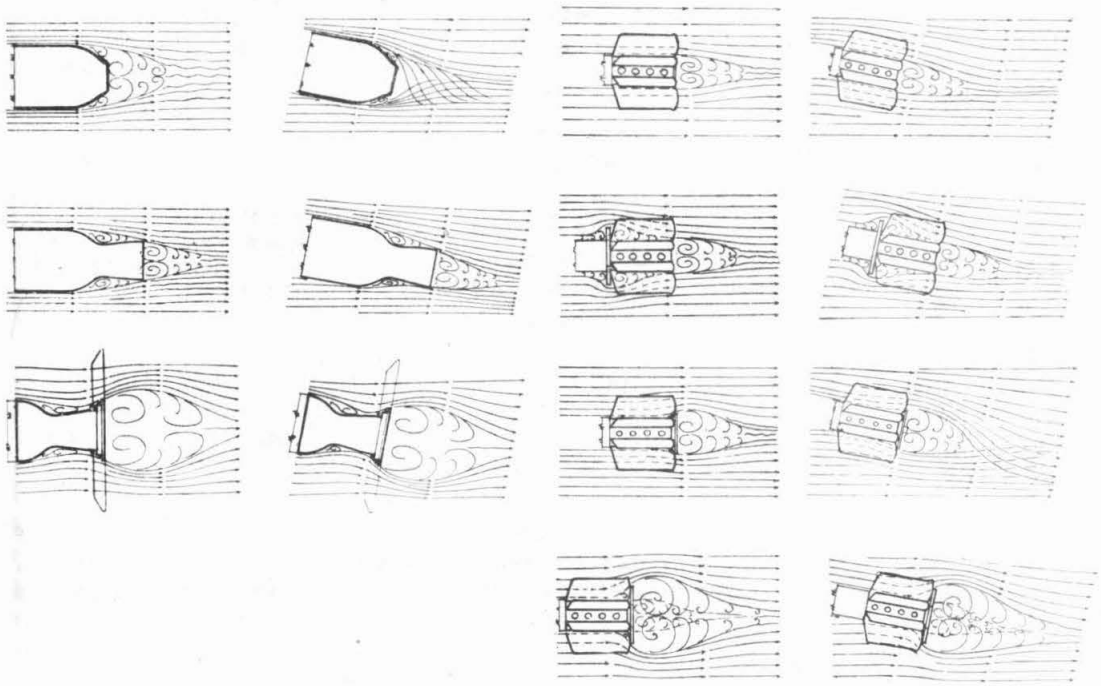

FIG. 39 – FLOW DIAGRAMS FOR A GROUP OF BLUNT AFTERBODY AND TAIL COMPONENTS

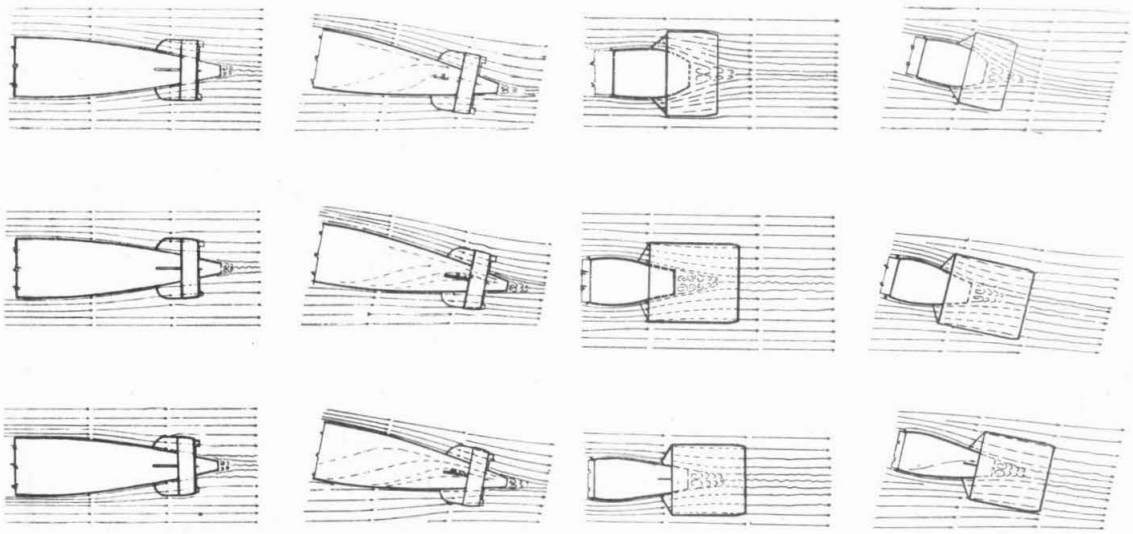

FIG. 40 – FLOW DIAGRAMS FOR A GROUP OF AFTERBODIES WITH RING TAILS

projectile such as a torpedo, and in Figure 37 for a stable projectile.

3. For a projectile with propellers, such as a torpedo, the damping forces are increased by the propellers. This is due, in part at least, to the increase in velocity between the fluid and the afterbody and tail structure.

4. A reasonable estimate of the damping effect of the tail structure can be secured by using the static test results to determine the cross force acting on the tail and by calculating the change in effective yaw angle at the tail due to the angular velocity. Curves such as Figures 36 and 37 can then be calculated for the projectile.

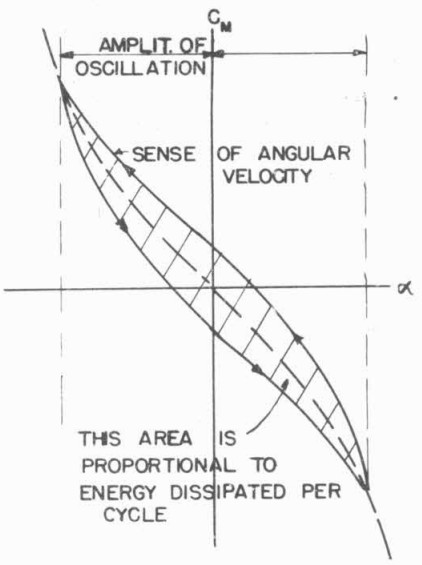

FIG. 37 — DETAILS OF HYSTERESIS LOOP FOR STABLE PROJECTILES

e. Flow Diagrams

One of the routine tests made on every new shape which came to the Laboratory was the determination of the flow pattern. Thus, the Laboratory has collected a large number of these flow diagrams

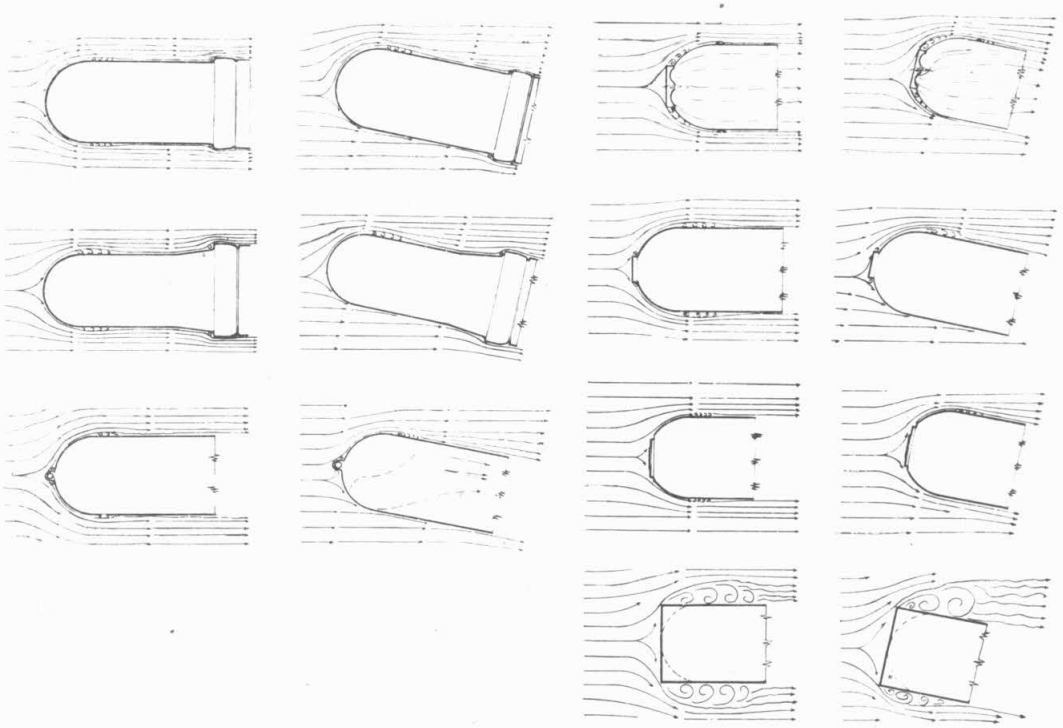

FIG. 38 — FLOW DIAGRAMS FOR A GROUP OF NOSE COMPONENTS

on many different shapes. In order to assist the projectile designer in visualizing the possible flow pattern on new projectiles, these flow diagrams have been presented in a group of systematic series of projectile components. This collection was presented in Report Section No. 6.1-sr207-1649. A few typical diagrams are shown in Figures 38 to 40.

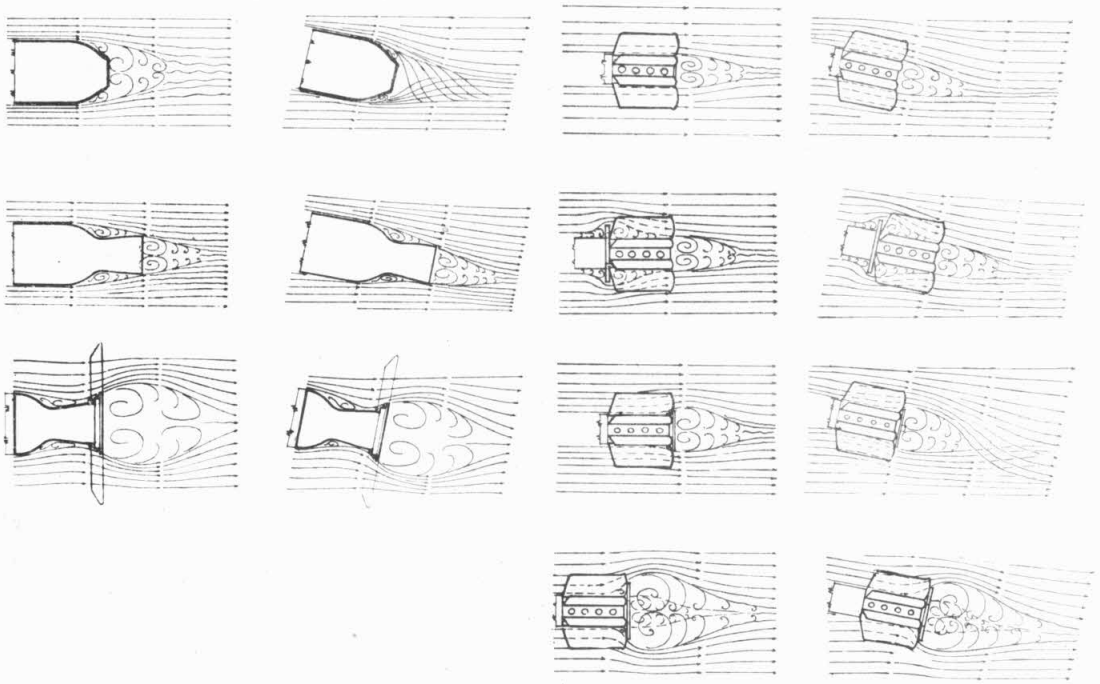

FIG. 39 – FLOW DIAGRAMS FOR A GROUP OF BLUNT AFTERBODY AND TAIL COMPONENTS

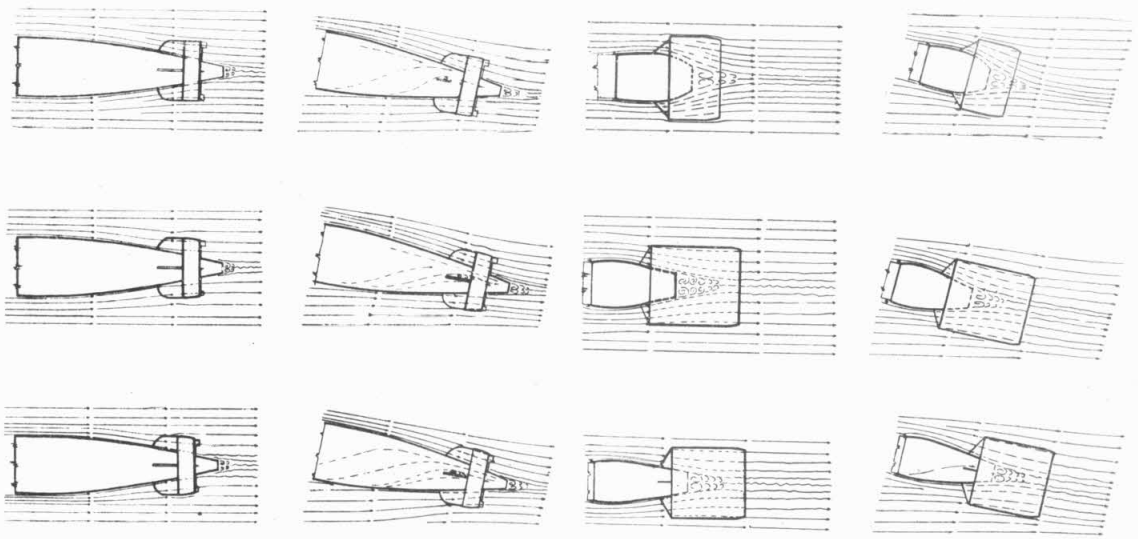

FIG. 40 – FLOW DIAGRAMS FOR A GROUP OF AFTERBODIES WITH RING TAILS

f. Cavitation and Noise

The first study carried out in the Laboratory which involved the investigation of cavitation phenomena had as its objective the determination of the relationship between cavitation and the production of noise by an underwater projectile. Such studies were made possible in the High Speed Water Tunnel by the fact that the tunnel is comparatively quiet in the sound band above 6,000 cycles, i.e., the supersonic field although it produces quite a lot of noise in the audible range. This matched very well with the needs of the study, since the main interest in the noise produced by cavitation was in the frequency band lying above 10,000 cycles. Considerable work has been done on this subject and two reports have been presented; Reports Section Nos. 6.1-sr207-924 and 6.1-sr207-1910.

The principal conclusions from these studies are:

1. Measurements of the variation in sound emitted in the 20-100 kc band with the beginning and growth of cavitation on four different projectile shapes show:

a. With the appearance of the slightest trace of cavitation the acoustic pressure increases to several times the magnitude of the background noise measured without cavitation.

b. The maximum noise is measured when the zone of cavitation is limited to a very narrow band of very small bubbles.

c. With further growth of cavitation the measured noise level drops gradually to approximately its initial value.

d. The more abrupt the projectile profile, the more abrupt the increase in noise as cavitation begins.

e. Cavitation which forms and collapses on the surface of the projectile causes the maximum noise at a value of the cavitation parameter K very close to the inception point, while for cavitation which collapses in water away from the projectile surface, some additional reduction in K is necessary to cause maximum noise.

2. For the hemisphere nose the maximum noise intensity measured in any frequency band is approximately proportional to the velocity.

3. Measurements to show the location of the noise sources indicate:

a. The main sound source is in the region of the trailing edge of the cavitation zone where the vapor bubbles are collapsing.

b. The source moves downstream as the zone of bubbles develops.

c. If the cavitation vapor bubbles are entrained and swept downstream before collapsing, the noise level drops.

Figure 41 shows the growth of cavitation on a hemispherical nose, and Figure 42 presents the relationship between the noise level and the cavitation parameter for the same series of tests. Figures 43 and 44 give the comparative performance for a truncated hemispherical nose.

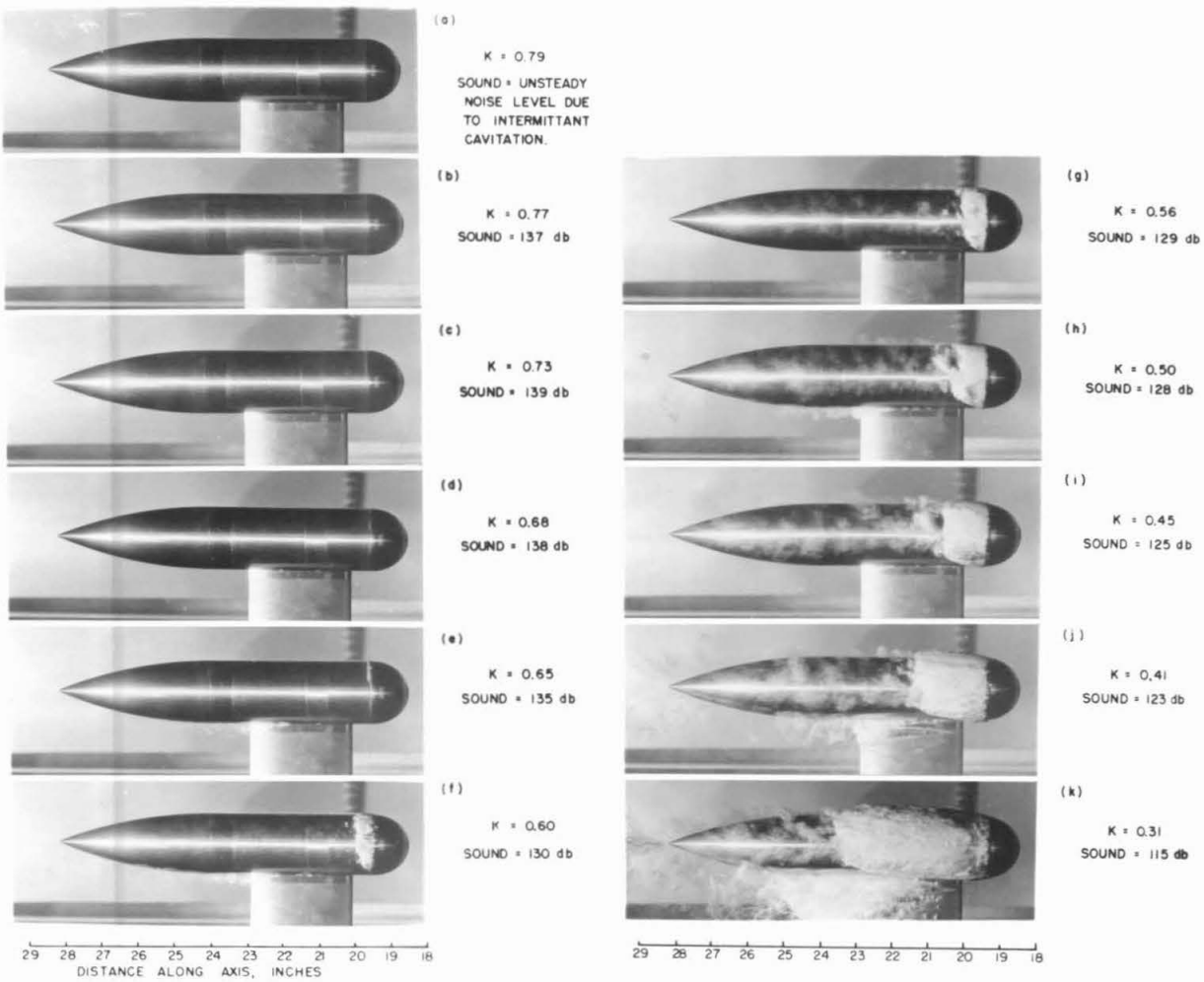

FIG. 41 — GROWTH OF CAVITATION ON A BODY WITH HEMISPHERICAL NOSE

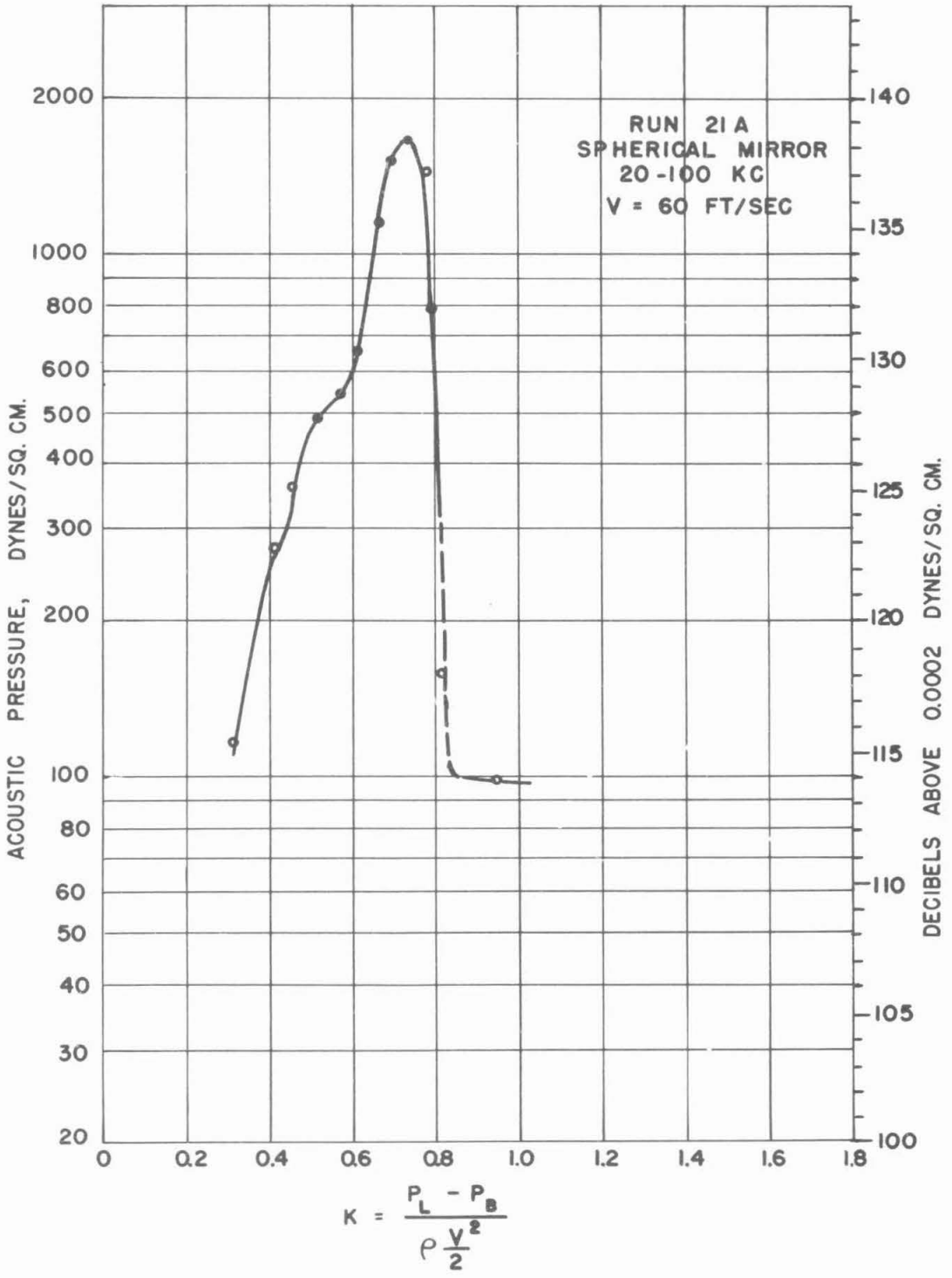

FIG. 42 — RELATIONSHIP BETWEEN NOISE LEVEL AND CAVITATION FOR HEMISPHERE

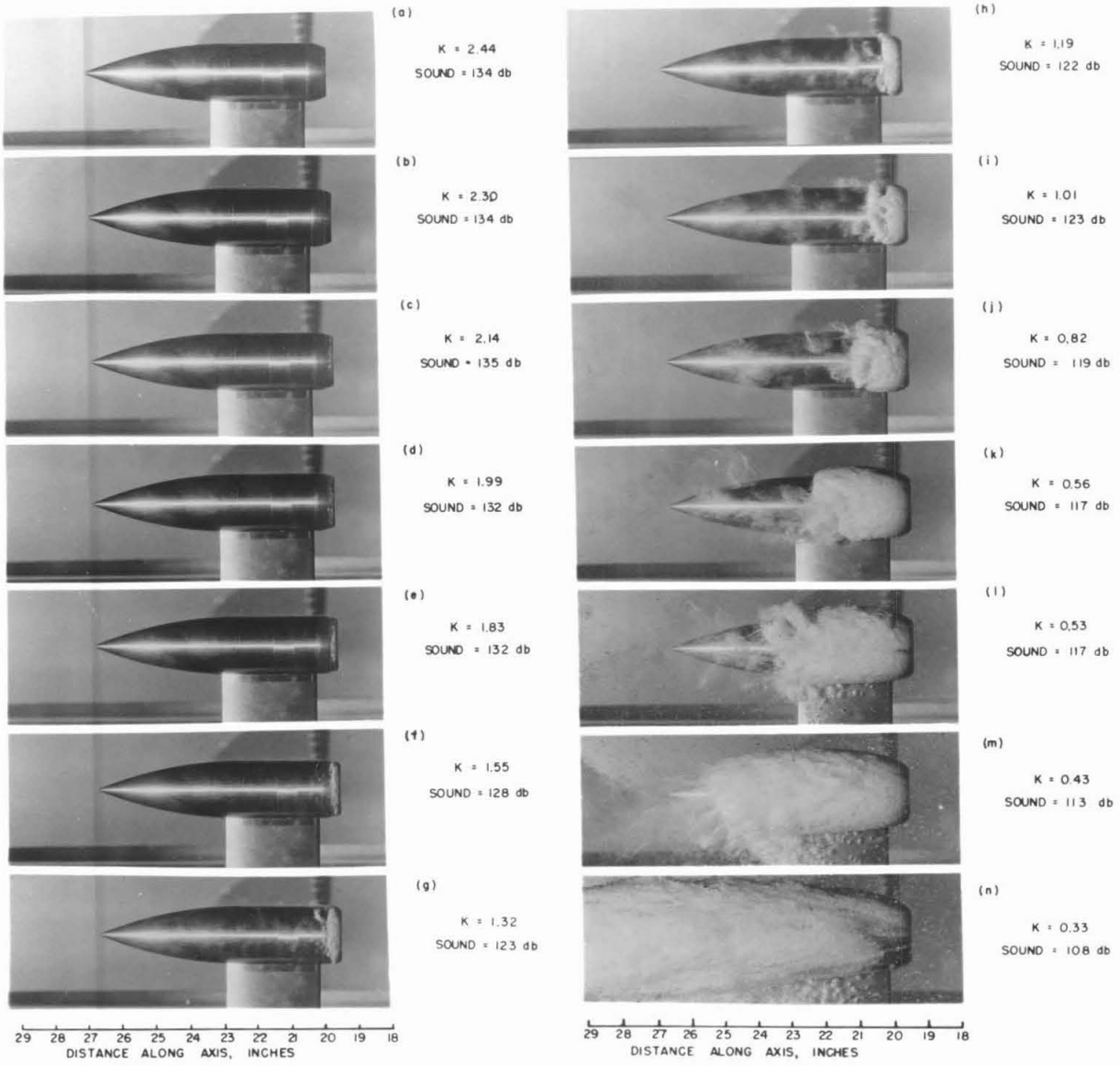

FIG. 43 — GROWTH OF CAVITATION ON BODY WITH TRUNCATED HEMISPHERE

g. Effect of Nose Shape on Cavitation Resistance

The next stage in the investigation of cavitation phenomena was to endeavor to develop shapes for projectile components which would be sufficiently cavitation-resistant so that the projectile would be cavitation-free under normal operating conditions. All of this cavitation work was, of course, in conjunction with the study of underwater projectiles and much of it specifically referred to torpedoes. It was found that for most projectile shapes,

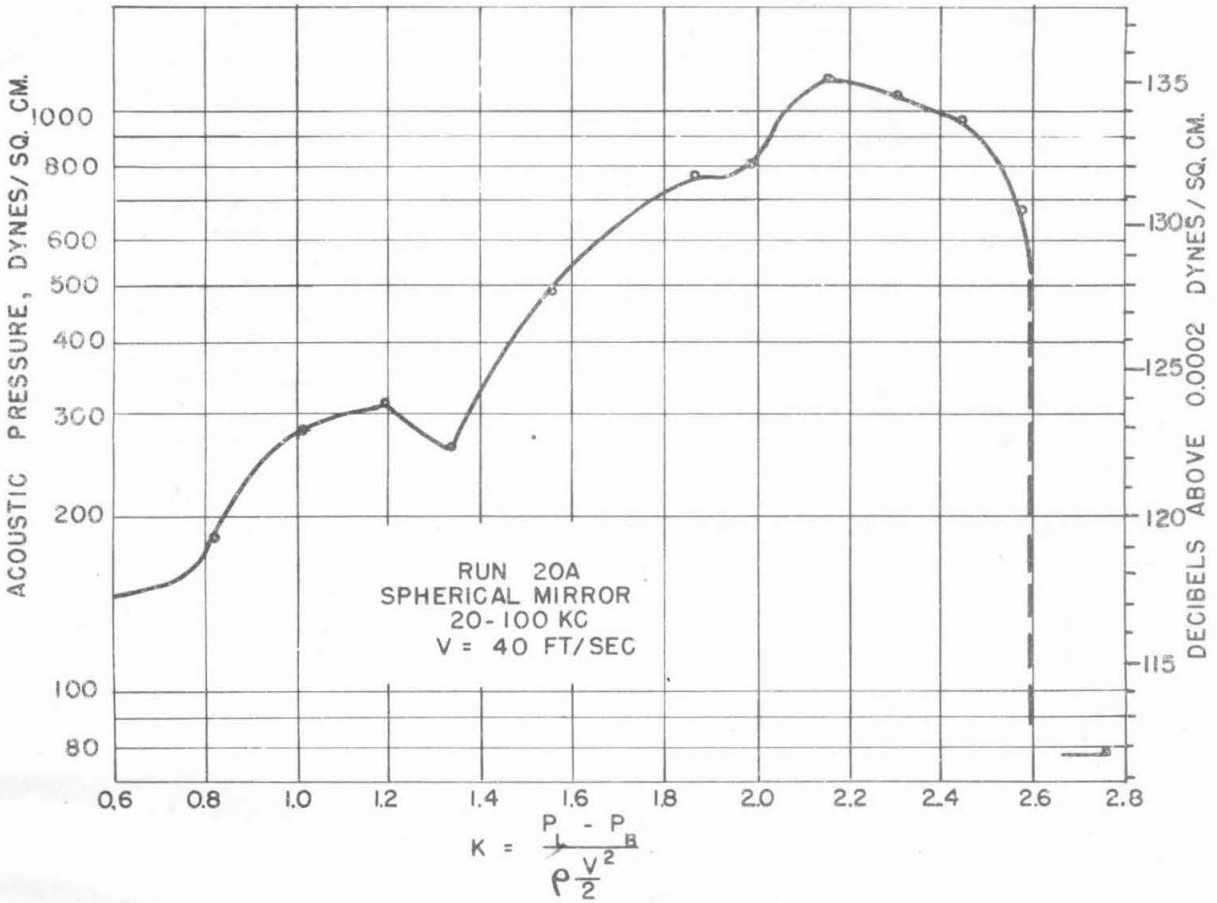

FIG. 44 — RELATIONSHIP BETWEEN NOISE LEVEL AND CAVITATION FOR TRUNCATED HEMISPHERE

cavitation first appeared on the nose. Therefore, a rather extensive study was made of the cavitation resistance of various nose shapes. Reports containing portions of these results are:

Laboratory No. ND-8.1

Section No. 6.1-sr207-1909

Section No. 6.1-sr207-1906

These studies have by no means covered the available ranges of shapes nor have they made possible the formulation of all of the basic principles involved in the relation between nose shape and cavitation resistance. However, the following points seem to be established:

1. Since cavitation is an evidence of low pressure it never appears on the portion of the nose of a projectile that produces a radially outward acceleration of the flow, but is only possible in regions on the nose or on other projectile components in which radially inward accelerations take place.

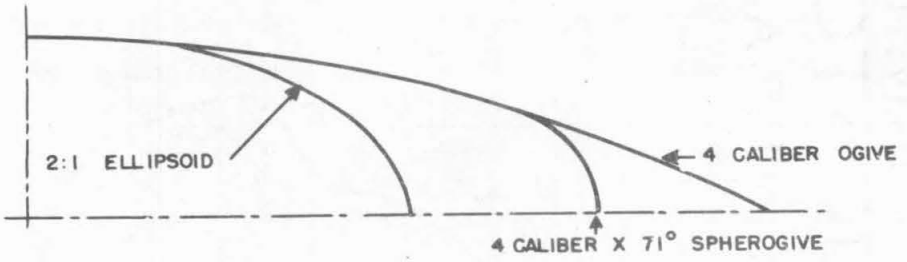

FIG. 45 – OUTLINE OF THREE NOSE SHAPES
ALL HAVING THE SAME CAVITATION RESISTANCE

2. Shapes causing high radially inward accelerations have low cavitation resistance.

3. As cavitation progresses from the incipient to the fully developed stage, the front edge of the cavitation zone moves forward or upstream, unless its point of origin is a geometric discontinuity. See Figures 41 and 43.

4. Other factors being equal, the drag force acting on a nose operating under full cavitation is proportional to the diameter of the cavity produced.

5. Ogives and ellipsoids have approximately the same cavitation resistance if the radius of curvature at the point of tangency to the cylindrical body is the same for both shapes. This is also true for a spherogive if the spherical segment is smaller than the size at which cavitation appears on the spherical portion before it does on the ogive. Figure 45 shows 3 such shapes, all of which have the same cavitation resistance.

6. The yawing of projectiles having hemispherical noses or noses having spherical segment tips of such dimensions that cavitation starts first on the spherical surface, appears to have no effect on the shape and character of the fully developed cavitation bubble for yaw angle up to the value at which some other element of the projectile touches the bubble wall. Force measurements made on projectiles within fully developed cavitation cavities confirm the fact that the forces acting on such noses are likewise independent of the yaw. For noses of other shapes a change of the yaw angle affects both the shape of the cavitation bubble and the forces acting on the nose. A comparison of Figure 46 and Figure 47 shows this difference in behavior.

7. The following performance characteristics have been found to apply to ogive and spherogive noses:

a. The incipient cavitation parameter, K_i, for ogive noses drops rapidly as the ogive radius is increased from 0.5 caliber to 1.0 caliber, the decrease being much less pronounced for radii between 1.0 caliber and 8.0 calibers.

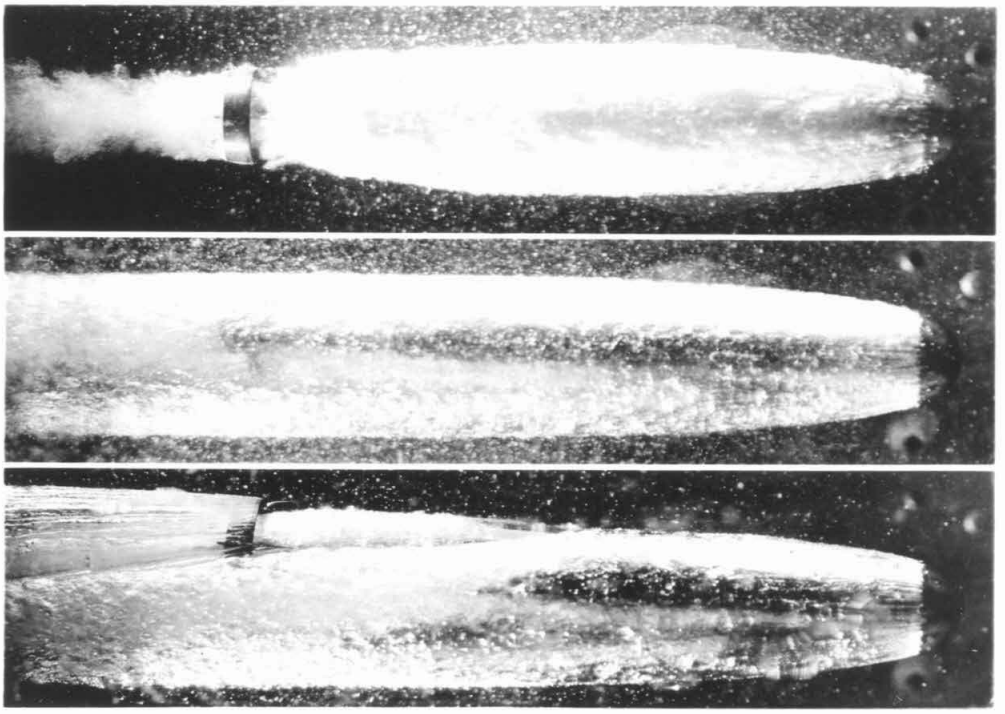

YAW = 0°
K = 0.22

YAW = 3°
K = 0.22

YAW = 6°
K = 0.23

FIG. 46 – EFFECT OF YAW ON THE CAVITATION BUBBLE PRODUCED BY A HEMISPHERE NOSE

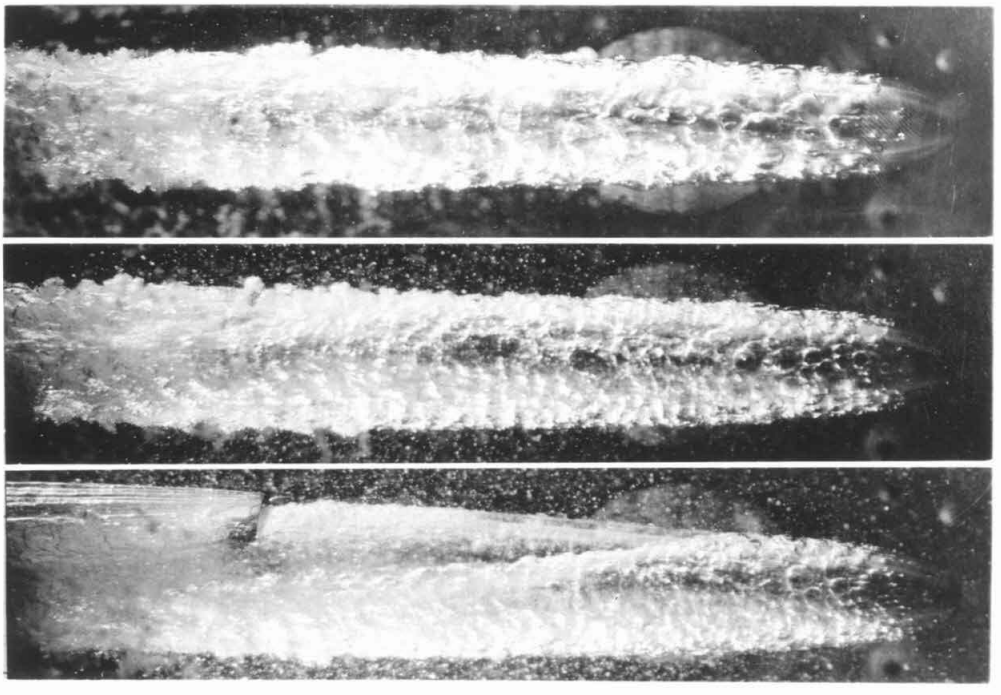

YAW = 0°
K = 0.16

YAW = 3°
K = 0.17

YAW = 6°
K = 0.17

FIG. 47 – EFFECT OF YAW ON THE CAVITATION BUBBLE PRODUCED BY AN ELLIPSOIDAL NOSE

b. The radius of the ogive drawn to the forward edge of a well developed cavitation bubble makes an angle of approximately 86° with the axis of the nose. This angle seems to be constant for all noses investigated.

c. The incipient cavitation parameter, K_i, increases rapidly with an increase in yaw angle. For a hemispherical nose K_i increases from 0.75 for zero yaw to 1.01 for 6° yaw.

d. When the sphere segment angle on a spherogive nose is large, cavitation occurs first on the sphere so that the inception and subsequent growth of the cavitation bubble depend only on the sphere size. When the sphere segment angle is small, cavitation occurs first on the ogive and the inception and subsequent bubble growth depend on the ogive and are independent of the sphere size. The critical sphere size dividing the two behaviors is different for different spherogive families. For the 5.0 caliber family of spherogives, this critical sphere size corresponds to a half-sphere angle (θ) of about 72°, and for the 1.0 caliber family, this angle is about 60°.

e. For a given family of spherogives, based on a constant ogive radius, the value of K for incipient cavitation (K_i) will be determined by the half spherical angle. The more blunt the nose, the higher the value of K_i.

h. Cavitation and Entrance Bubbles

During the water-entry phase of aircraft torpedoes and similar projectiles, the behavior of the projectile in the air bubble that surrounds it is of major importance in determining the trajectory. A detailed consideration of this field made it obvious that there were many points of similarity between these entrance bubbles and the voids or vapor bubbles produced when a projectile is operated under conditions of severe cavitation. The evidence available from the many studies made in the Water Tunnel of the behavior of different projectile shapes under conditions of heavy cavitation were formulated and presented in Report Section No 6.1-sr207-1900. The following points summarize the major similarities and differences that are believed to exist between cavitation and entrance bubbles.

1. For a given projectile, the value of the cavitation parameter is characteristic of the size and shape of the bubble, irrespective of whether the bubble is filled with air or water vapor. In calculating the cavitation parameter for the entrance bubble, the actual gas pressure inside of the bubble must be used instead of the vapor pressure of the water.

2. Cavitation and entrance bubbles both form in low pressure regions on the projectile.

Although cavitation bubbles often appear foam-filled, they are usually clear gas spaces as are entrance bubbles. The

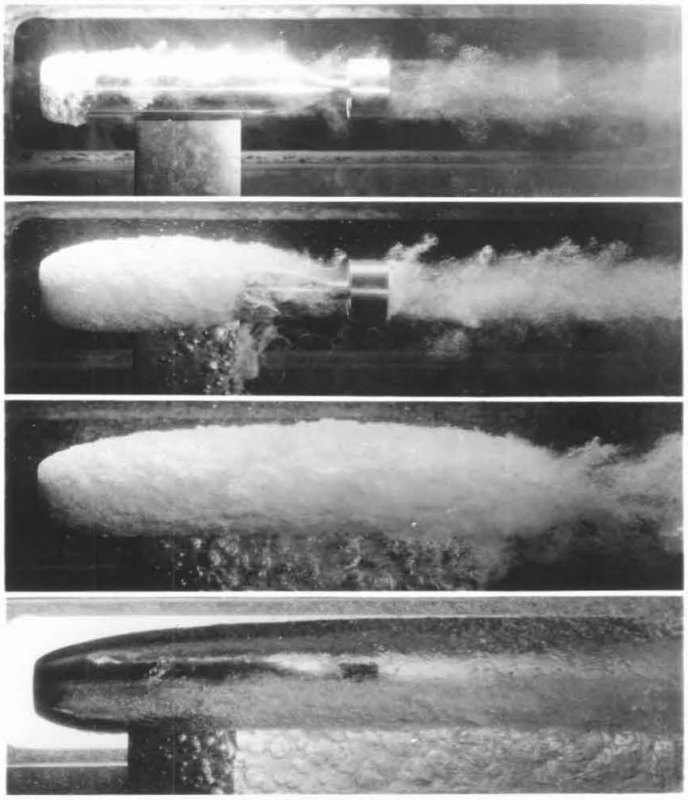

FIG. 48 – DEVELOPMENT OF CAVITATION BUBBLE

foamy appearance is due to the violent boiling or vaporization at the surface of the bubble. Figure 48 shows the development of a cavitation bubble. It illustrates the foamy appearance but also shows that, when the cavitation bubble is fully developed, at least the forward part of it becomes clear and transparent, with no traces of foam inside.

3. Gas is entrained and removed from either type of bubble by the rapidly moving liquid surrounding it. Figure 49 shows an example of the entrainment.

4. The entrance bubble is inherently transient in character since its gas supply continues only up to the instant that the rear of the bubble closes. From then on, the bubble decays due to the entrainment of the gases.

5. Since the gas supply for the cavitation bubble comes from the evaporation of the surrounding liquid and is therefore, limitless, this type of bubble may exist in a steady state condition, as for example, on a torpedo moving with a constant velocity at a constant depth.

6. The geometric shape of the projectile determines, for a given value of the cavitation parameter, not only the shape of the bubble, but also the drag force on the projectile while it is surrounded by the bubble, and the magnitude and rate of change with yaw of the cross force and moment acting on it.

i. Outlines of Important Problems Still Unsolved

It is obvious that there will always be many specific problems which must be studied to secure satisfactory designs for each new major projectile. However, there are certain general fields in which it is felt that further research would result in substantial progress that would be of use to all those interested in underwater ordnance. Some of the principal fields are:

1. Further investigations of dynamic stability and damping. This can be studied in water tunnels by use of dynamic balances.

2. The systematic study of optimum design of stabilizing surfaces for streamlined controllable projectiles, such as torpedoes.

3. Spectrum analysis of the sound produced by cavitation and an investigation of the possible existence of a "scale-effect" in cavitation measurements.

4. Effects of various types of jet and propeller propulsion on the stability and performance characteristics of torpedoes.

5. The systematic development of projectile shapes having high cavitation resistance that will permit of high-speed, low-submergence underwater operation.

6. The analysis of the causes and effects of the forces acting on an air-launched underwater projectile during the entry phase.

7. The evaluation of the effects of scale on the testing of water-entry phenomena.

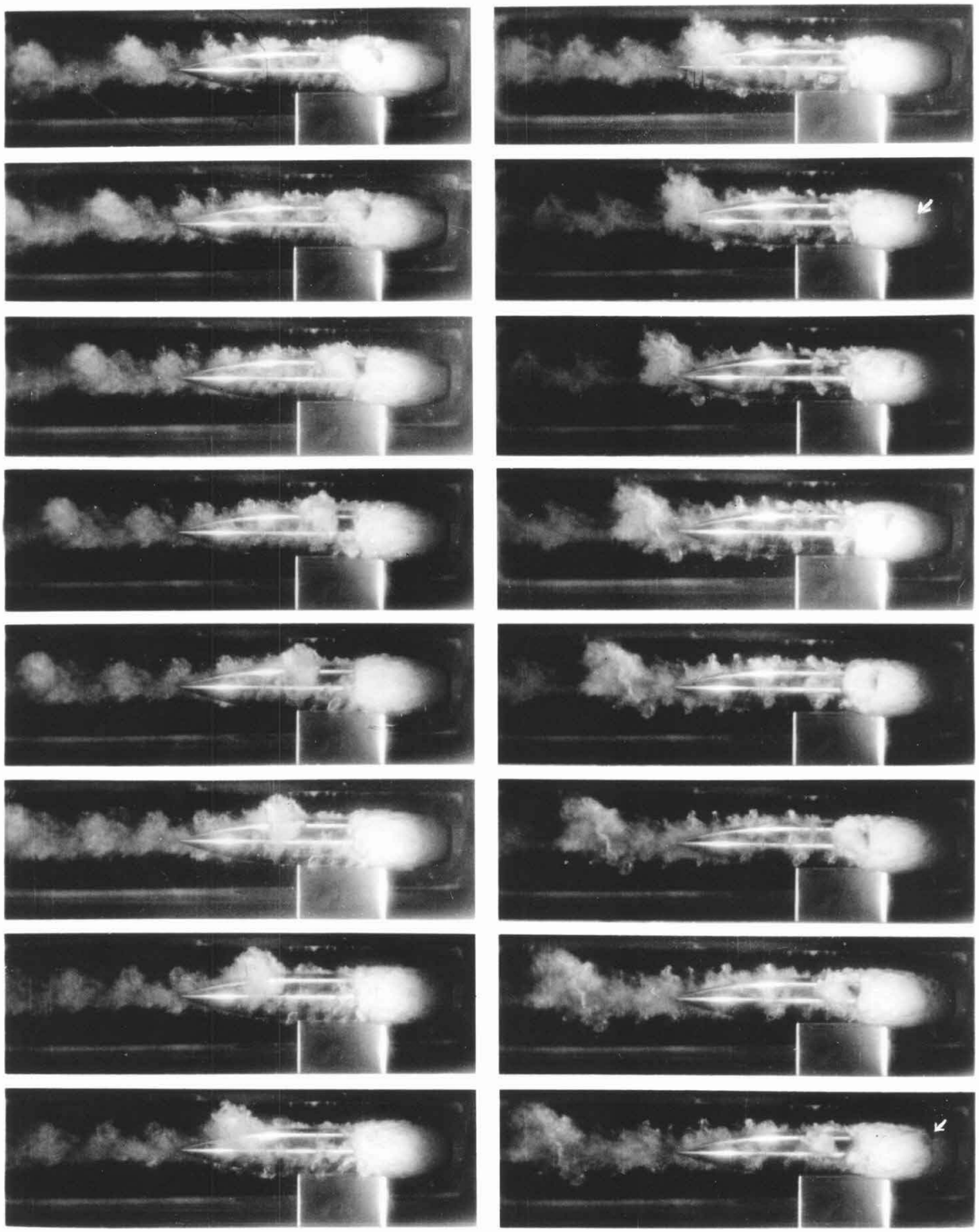

FIG. 49 – ENTRAINMENT FROM CAVITATION BUBBLE

APPENDIX 1

LIST OF REPORTS ISSUED UNDER CONTRACT OEMsr-207

Projectile 61

"Memorandum on Preliminary Water Tunnel Tests of Projectile 61," ND-8, Robert T. Knapp, CIT, November 7, 1942.

"Memorandum on Observation of Cavitation on Projectile 61," ND-8.1, Robert T. Knapp, CIT, November 24, 1942.

"Underwater Performance Characteristics of Projectile 61.02," OSRD No. 6.1-sr207-925, Robert Peabody, CIT, August 15, 1944.

"Underwater Performance Characteristics of Projectiles 61.01 and 61.03," OSRD No. 6.1-sr207-1645, Joseph Levy, CIT, June 29, 1944.

"Underwater Characteristics of Projectile 61.04," OSRD No. 6.1-sr207-1653, Robert Peabody, CIT, September 26, 1944.

Mark 13 and Mark 25 Torpedoes

"Water Tunnel Tests of the Mark 13-1, Mark 13-2, and Mark 13-2A Torpedoes," OSRD No. 6.1-sr207-936, Robert T. Knapp, CIT, November 9, 1943.

"Water Tunnel Tests of the Mark 13-1, Mark 13-2, and Mark 13-2A Torpedoes with Shroud Ring Tails," OSRD No. 6.1-sr207-939, Joseph Levy, CIT, November 24, 1943.

"Water Tunnel Tests of the Mark 13 Torpedo with Spade and Stabilizer Ring Noses," OSRD No. 6.1-sr207-1278, Harold Doolittle, CIT, June 5, 1944.

"Pressure Distribution Measurements on the Mark 13-1, 13-2, and 13-2A Torpedoes," OSRD No. 6.1-sr207-1643, Joseph Levy, CIT, June 23, 1944.

"Mark 13-1 Torpedo with Various Noses," OSRD No. 6.1-sr207-1909, Harold Doolittle, CIT, February 1, 1945.

"Underwater Performance Characteristics of the Mark 13-2A Torpedo with Suspension Fittings," OSRD No. 6.1-sr207-1650, Joseph Levy, CIT, August 18, 1944.

"Pressure Distribution on the Mark 13 Series Torpedoes with Shroud Ring Tail," OSRD No. 6.1-sr207-1905, Joseph Levy, CIT, January 15, 1945.

"Force Tests of Mark 13-1 Torpedo with Suspension Bands," OSRD No. 6.1-sr207-2231, Gerald Robison, CIT, May 17, 1945.

"Water Tunnel Tests of the Mark 25 Torpedo with Gas Exhaust through a Vertical Fin," OSRD No. 6.1-sr207-1275, Harold Doolittle, CIT, May 8, 1944.

"Water Tunnel Tests of the Mark 25 Torpedo with a Horizontal Exhaust Pipe," OSRD No. 6.1-sr207-1640, Harold Doolittle, CIT, June 5, 1944.

"Water Tunnel Tests of the Mark 25 Torpedo with Expanding Exhaust Pipe," OSRD No. 6.1-sr207-1642, Harold Doolittle, CIT, June 20, 1944.

"Mark 25 Torpedo Exhaust Gas Investigation," OSRD No. 6.1-sr 207-1916, Harold Doolittle, CIT, April 12, 1945.

"Mark 25 Torpedo with Various Exhaust Pipes," OSRD No. 6.1-sr 207-2236, Harold Doolittle, CIT, July 14, 1945.

"Pressure Distribution Measurements on the Mark 25 Torpedo," OSRD No. 6.1-sr207-2248, Joseph Levy, CIT, August 31, 1945.

Mark 14 and 15 and Mark 26 Torpedoes

"Force and Cavitation Tests, Mark 14-1 and Mark 15-1 Torpedoes," OSRD No. 6.1-sr207-2238, Joseph Levy, CIT, July 15, 1945.

"Pressure Distribution Measurements on the Mark 14-1 and Mark 15-1 Torpedoes," OSRD No. 6.1-sr207-2244, Joseph Levy, CIT, August 15 1945.

"Force and Cavitation Tests on the Mark 26 Torpedo," OSRD No. 6.1-sr207-2249, Robert Peabody, CIT, August 31, 1945.

Hydrobombs

"Water Tunnel Tests of the Hydrobomb," OSRD No. 6.1-sr207-1276, Harold Doolittle, CIT May 13, 1944

"Force and Cavitation Tests - Westinghouse Hydrobomb," OSRD No. 6.1-sr207-2234, Robert Peabody, CIT, June 27, 1945.

"Force Tests of the United Shoe Machinery No. 8 Hydrobomb," OSRD No 6.1-sr207-2247, Gerald Robison, CIT, August 23, 1945.

Cavitation and Sound

"Entrance and Cavitation Bubbles," OSRD No. 6.1-sr207-1900, Robert T. Knapp, CIT, December 27, 1944.

"Nose Cavitation - Ogives and Spherogives," OSRD No. 6.1-sr207-1906, Harold Doolittle, CIT, January 18, 1945.

"Hydrodynamic Forces Resulting from Cavitation," OSRD No. 6.1-sr207-2242, James W. Daily, CIT, July 21, 1945.

"Measurements of High Frequency Noise Produced by Cavitating Projectiles in the High Speed Water Tunnel," OSRD No. 6.1-sr 207-924, Robert T. Knapp, CIT, August 20, 1943.

"Cavitation Noise from Underwater Projectiles," OSRD No. 6.1-sr 207-1910, James W. Daily and Howard Baller, CIT, March 20, 1945.

Squid

"Water Tunnel Tests of the British Squid - Projectile Type 'C'", OSRD No. 6.1-sr207-933, Robert T. Knapp, CIT, October 29, 1943.

"Water Tunnel Tests of the British Squid - Projectile Type 'C' with Two Alternate Flat Noses," OSRD No. 6.1-sr207-938, Harold Doolittle, CIT, November 29, 1943.

"Drag Tests of the British Squid," OSRD No. 6.1-sr207-1904, Gerald Robison, CIT, January 8, 1945.

"Force Tests of Squid with New Afterbody, Tails, and Noses," OSRD No. 6.1-sr207-2243, Gerald Robison, CIT, July 30, 1945.

Rockets

"Memorandum on Water Tunnel Tests of a 21-3/8" Rocket Projectile, ND-11," Robert T. Knapp, CIT, November 19, 1942.

"Memorandum on Water Tunnel Tests of a 2.37" Rocket Projectile with Collapsible Type Tails," OSRD No. 6.1-sr207-1314, Robert T. Knapp, CIT, January 20, 1943.

"Memorandum of Water Tunnel Tests of a 2.37" Rocket Projectile with Hemispherical Noses and Ring Tails," OSRD No. 6.1-sr207-1303, Robert T. Knapp, CIT, February 19, 1943.

"Water Tunnel Tests of the M-7, 2.36" A.T. Rocket," OSRD No. 6.1-sr207-276, Robert T. Knapp, CIT, June 26, 1943.

"Water Tunnel Tests of the M-6, 2.36" A.T. Rocket," OSRD No. 6.1-sr207-920, Robert T. Knapp, CIT, July 20, 1943.

"Water Tunnel Tests of the M-6, 2.36" A.T. Rocket with Five Designs of Shroud Ring Tail," OSRD No. 6.1-sr207-934, Robert T. Knapp, CIT, November 4, 1943.

"Memorandum of Water Tunnel Tests of the 2-1/4" A.A. Rocket Projectile, ND-13," Robert T. Knapp, CIT, May 14, 1943.

"Water Tunnel Tests of the 2-1/4" A.A. Rocket Projectile," OSRD No. 6.1-sr207-927, James W. Daily, CIT, December 28, 1943.

"Memorandum of Water Tunnel Tests of a 4.5" Rocket Projectile," OSRD No. 6.1-sr207-1312, Robert T. Knapp, CIT, February 22, 1943.

"Water Tunnel Tests of the 4.5" Rocket Projectile with Three Different Fin Tails and One Ring Type Tail," OSRD No. 6.1-sr 207-1304, Robert T. Knapp, CIT, May 28, 1943.

"Force Tests of the 4.5" Rocket, T38E3," OSRD No. 6.1-sr207-1919, Gerald Robison, CIT, May 1, 1945.

"Water Tunnel Tests of the 3.5" Rotating Rocket," OSRD No. 6.1-sr207-1270, Harold Doolittle, CIT, April 21, 1944.

"3.5" Rotating Rocket with Various Afterbodies," OSRD No. 6.1-sr207-1903, Harold Doolittle, CIT, January 4, 1945.

"Water Tunnel Tests of the 7.2" Chemical Rocket," OSRD No. 6.1-sr207-1261, Harold Doolittle, CIT, December 22, 1943.

"Tests of Four Models of the 5" SSR Rotating Rocket," OSRD No. 6.1-sr207-2239, Harold Doolittle, CIT, July 24, 1945.

"Water Tunnel Tests of the 15 CM German Spinner Rocket," OSRD No. 6.1-sr207-932, Robert T. Knapp, CIT, November 11, 1943.

"Tests of 5" HVAR Projectile with Fin and Ring Tails," OSRD No. 6.1-sr207-2241, Harold Doolittle, CIT, August 20, 1945.

Bombs

"Memorandum on Water Tunnel Tests of the AN-Mark 41 Bomb," OSRD No. 6.1-sr207-735, Robert T. Knapp, CIT, March 31, 1943.

"Force Tests of Concrete Practice Bombs, M38A2 Practice Bomb, AN-M43 G.P. 500 lb Bomb, AN-M56 L.C. 4000 lb Bomb," OSRD No. 6.1-sr207-2245, Robert Peabody, CIT, August 14, 1945.

"Force and Cavitation Tests on the Mark 53 Aircraft Depth Bomb," OSRD No. 6.1-sr207-2350, Harold Doolittle, CIT, August 31, 1945.

Miscellaneous

"The High Speed Water Tunnel at the California Institute of Technology," OSRD No. 6.1-sr207-165, Robert T. Knapp, V. A. Vanoni, J. W. Daily, CIT, Jnly 3, 1942.

"Water Tunnel Tests of the 60 MM Mortar Projectile," OSRD No. 6.1-sr207-926, Robert T. Knapp, CIT, September 2, 1943.

"Memorandum on Water Tunnel Tests of 2" Diameter Projectiles with Hemispherical Noses and Square Ends," ND-10, Robert T. Knapp, CIT, November 10, 1942.

"Measurements of Fluid Friction Loss in O.50 Caliber Gun Barrels," OSRD No. 6.1-sr207-279, Robert T. Knapp, CIT, August 20, 1943.

"Force and Cavitation Characteristics of the NACA 4412 Hydrofoil," OSRD No. 6.1-sr207-1273, James W Daily, CIT, June 10, 1944.

"Flow Diagrams of Projectile Components," OSRD No. 6.1-sr207-1649, Garrett Van Pelt, Elizabeth Thorne, CIT, September 15, 1944.

APPENDIX 2

DEFINITIONS

YAW ANGLE, ψ

The angle, in a horizontal plane, which the axis of the projectile makes with the direction of motion. Looking down on the projectile, yaw angles in a clockwise direction are positive (+) and in a counterclockwise direction, negative (−).

PITCH ANGLE, α

The angle, in a vertical plane, which the axis of the projectile makes with the direction of motion. Pitch angles are positive (+) when the nose is up and negative (−) when the nose is down.

LIFT, L

The force, in pounds, exerted on the projectile normal to the direction of motion and in a vertical plane. The lift is positive (+) when acting upward and negative (−) when acting downward.

CROSS FORCE, C

The force, in pounds, exerted on the projectile normal to the direction of motion and in a horizontal plane. The cross force is positive when acting in the same direction as the displacement of the projectile nose for a positive yaw angle, i.e., to an observer facing in the direction of travel, a positive cross force acts to the right.

DRAG, D

The force, in pounds, exerted on the projectile parallel with the direction of motion. The drag is positive when acting in a direction opposite to the direction of motion.

MOMENT, M

The torque, in foot pounds, tending to rotate the projectile about a transverse axis. Yawing moments tending to rotate the projectile in a clockwise direction (when looking down on the projectile) are positive (+), and those tending to cause counterclockwise rotation are negative (−). Pitching moments tending to rotate the projectile in a clockwise direction (when looking at the projectile from the port side) are positive (+), and those tending to cause counterclockwise rotation are negative (−).

In accordance with this sign convention a moment has a destabilizing effect when it has the same sign as the yaw angle or pitch angle, and a stabilizing effect when the moment and yaw or pitch angle have opposite signs

NORMAL COMPONENT, N

The sum of the components of the drag and cross force (or lift) acting normal to the axis of the projectile. The value of the normal component is given by the following:

$$N = D \sin \psi + C \cos \psi \qquad (1)$$

or

$$N = D \sin \alpha + L \cos \alpha \qquad (1a)$$

in which

N = Normal component in lbs

D = Drag in lbs

C = Cross force in lbs

L = Lift force in lbs

ψ = Yaw angle in degrees

α = Pitch angle in degrees

CENTER OF PRESSURE, CP

The point in the axis of the projectile at which the resultant of all forces acting on the projectile is applied.

CENTER-OF-PRESSURE ECCENTRICITY, e

The distance between the center of pressure (CP) and the center of gravity (CG) expressed as a decimal fraction of the length (l) of the projectile. The center-of-pressure eccentricity is derived as follows:

$$e = (l_{cp} - l_{cg}) \frac{1}{l} = \frac{1}{l} \frac{M_{cg}}{N} \qquad (2)$$

in which

e = Center-of-pressure eccentricity

l = Length of projectile in feet

l_{cg} = Distance from nose of projectile to CG in feet

l_{cp} = Distance from nose of projectile to CP in feet

COEFFICIENTS

The force and moment coefficients used are derived as follows:

Drag coefficient, $$C_D = \frac{D}{\rho \frac{V^2}{2} A_D} \quad (3)$$

Cross force coefficient, $$C_C = \frac{C}{\rho \frac{V^2}{2} A_D} \quad (4)$$

Lift coefficient, $$C_L = \frac{L}{\rho \frac{V^2}{2} A_D} \quad (5)$$

Moment coefficient, $$C_M = \frac{M}{\rho \frac{V^2}{2} A_D l} \quad (6)$$

in which

D = Measured drag force in lbs

C = Measured cross force in lbs

L = Measured lift force in lbs

ρ = Density of the fluid in slugs/cu ft = w/g

w = Specific weight of the fluid in lbs/cu ft

g = Acceleration of gravity in ft/sec^2

A_D = Area in sq ft at the maximum cross section of the projectile taken normal to the geometric axis of the projectile

V = Mean relative velocity between the water and the projectile in ft/sec

M = Moment, in foot-pounds, measured about any particular point on the geometric axis of the projectile

l = Overall length of the projectile in feet

REYNOLDS NUMBER

In comparing hydraulic systems involving only friction and inertia forces, a factor called Reynolds number is of great utility. This is defined as follows:

$$R = \frac{lV}{\nu} = \frac{lV\rho}{\mu} \qquad (7)$$

in which

R = Reynolds number

l = Overall length of projectile, feet

V = Velocity of projectile, feet per sec

ν = Kinematic viscosity of the fluid, sq ft per sec = μ/ρ

ρ = Mass density of the fluid in slugs per cu ft

μ = Absolute viscosity in pound-seconds per sq ft

Two geometrically similar systems are also dynamically similar when they have the same value of Reynolds number. For the same fluid in both cases, a model with small linear dimensions must be used with correspondingly large velocities. It is also possible to compare two cases with widely differing fluids provided l and V are properly chosen to give the same value of R.

CAVITATION PARAMETER

In the analysis of cavitation phenomena, the cavitation parameter has been found very useful. This is defined as follows:

$$K = \frac{P_L - P_B}{\rho \frac{V^2}{2}} \qquad (8)$$

in which

K = Cavitation parameter

P_L = Absolute pressure in the undisturbed liquid, lbs/sq ft

P_B = Vapor pressure corresponding to the water temperature, lbs/sq ft

V = Velocity of the projectile, ft/sec

ρ = Mass density of the fluid in slugs per cu ft = w/g

w = weight of the fluid in lbs per cu ft

g = acceleration of gravity

Note that any homogeneous set of units can be used in the computation of this parameter. Thus, it is often convenient to express this parameter in terms of the head, i.e.,

$$K = \frac{h_L - h_B}{\frac{V^2}{2g}} \qquad (9)$$

where

h_L = Submergence plus the barometric head, ft of water

h_B = Pressure in the bubble, ft of water

It will be seen that the numerator of both expressions is simply the net pressure acting to collapse the cavity or bubble. The denominator is the velocity pressure. Since the entire variation in pressure around the moving body is a result of the velocity, it may be considered that the velocity head is a measure of the pressure available to open up a cavitation void. From this point of view, the cavitation parameter is simply the ratio of the pressure available to collapse the bubble to the pressure available to open it. If the K for incipient cavitation is considered, it can be interpreted to mean the maximum reduction in pressure on the surface of the body measured in terms of the velocity head. Thus, if a body starts to cavitate at the cavitation parameter of one, it means that the lowest pressure at any point on the body is one velocity head below that of the undisturbed fluid.

The shape and size of the cavitation bubbles for a specific projectile are functions of the cavitation parameter. If P_B is taken to represent the gas pressure within the bubble instead of the vapor pressure of the water, as in normal investigations, the value of K obtained by the above formula will be applicable to an air bubble. In other words, the behavior of the bubble will be the same whether the bubble is due to cavitation, the injection of exhaust gas, or the entrainment of air at the time of launching.

The following chart gives values of the cavitation parameter as a function of velocity and submergence in sea water.

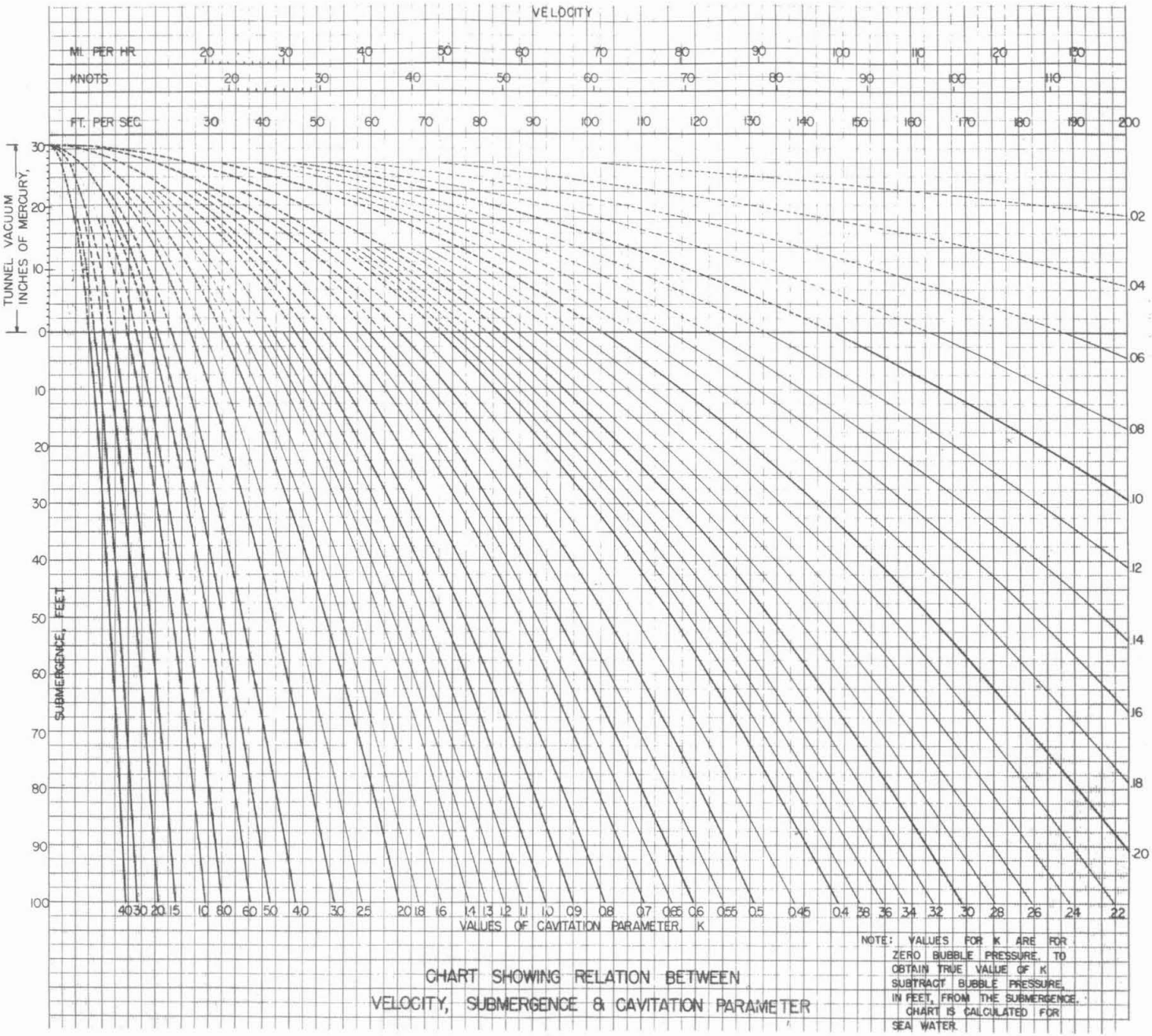

CHART SHOWING RELATION BETWEEN
VELOCITY, SUBMERGENCE & CAVITATION PARAMETER